Cooperation between ZEB2 and SP1 upregulates PD-L1 and CCL2 to promote the immunosuppressive activity of tumor cells

DONGJOON KO[1,2], YUNHEE LEE[1], JUNGHWA YOON[1], EUN KYOUNG CHOI[1], DONGHWAN JANG[1] and SEMI KIM[1,2]

[1]Microbiome Convergence Research Center, Korea Research Institute of Bioscience and Biotechnology, Daejon 34141, Republic of Korea; [2]Department of Functional Genomics, Korea University of Science and Technology, Daejon 34113, Republic of Korea

Received February 26, 2025; Accepted May 5, 2025

DOI: 10.3892/ijo.2025.5801

Abstract. Epithelial-mesenchymal transition (EMT) is implicated in tumor progression and EMT-inducing transcription factors play multifaceted roles; however, the molecular mechanisms underlying these processes are not well understood. Previously, we showed that ZEB2 acts cooperatively with the transcription factor SP1 to function as a transcriptional activator that promotes cancer cell invasion and survival, as well as angiogenesis. The present study reported a novel role for Zinc Finger E-Box Binding Homeobox 2 (ZEB2) in conferring immunosuppressive activity on cancer cells, as well as the underlying molecular mechanism. ZEB2 cooperated with SP1 to upregulate transcription of *CD274* and *CCL2* by interacting with the proximal SP1 element in their promoters. ZEB2-mediated programmed cell death 1 ligand 1 (PD-L1) upregulation on tumor cells inhibited T cell activation and cytokine secretion in a co-culture system. ZEB2 upregulated C-C motif chemokine ligand 2 (CCL2) secretion to promote migration of macrophages and drive polarization to an M2-like phenotype. ZEB2 suppressed the activity of tumor-infiltrating T cells in a syngeneic mouse tumor model. Furthermore, SUMOylation of ZEB2 by PC2 was required for efficient cooperation between ZEB2 and SP1, as well as for subsequent gene expression. Clinical data showed that *ZEB2* expression is associated positively with expression of *CD274* and *CCL2*. Expression of both *ZEB2* and *CD274* or *CBX4* has prognostic significance for predicting survival of colon cancer patients. The present study demonstrated a previously unrecognized role for ZEB2: Direct modulation of the interaction between tumor cells and immune cells. Taken together, the data increased our understanding of the molecular mechanism underlying immunosuppression mediated by an EMT-inducing transcription factor.

Correspondence to: Dr Semi Kim, Microbiome Convergence Research Center, Korea Research Institute of Bioscience and Biotechnology, 125 Gwahak-ro, Yuseong, Daejon 34141, Republic of Korea
E-mail: semikim@kribb.re.kr

Abbreviations: ELISA, enzyme-linked immunosorbent assay; EMT, epithelial-mesenchymal transition; ERK1/2, extracellular signal-regulated kinase 1/2; 293E, human embryonic kidney 293E; qPCR, quantitative polymerase chain reaction; siRNA, small interfering RNA; shRNA, short hairpin RNA; TCGA, The Cancer Genome Atlas; VEGF, vascular endothelial growth factor; PD-1, programmed cell death 1; PD-L1, PD-1 ligand 1; CCL2, C-C motif chemokine ligand 2; SUMO, small ubiquitin-like modifier; TME, tumor microenvironment; NFAT, nuclear factor of activated T cells

Key words: Zinc Finger E-Box Binding Homeobox 2, SP1, programmed cell death 1 ligand 1, C-C motif chemokine ligand 2, immunosuppression, SUMOylation

Introduction

Epithelial-mesenchymal transition (EMT) is a process implicated in tumor progression, as well as in physiological processes such as embryogenesis and epithelial tissue healing (1). EMT usually occurs during cancer cell invasion and dissemination, during which epithelial cells undergo morphological and molecular changes to acquire the motile properties of mesenchymal cells (2,3). These molecular changes are orchestrated (directly or indirectly) by EMT-inducing transcription factors (EMT-TFs), including members of the ZEB, SNAIL and TWIST families (4-6). These transcription factors induce EMT processes such as downregulation of E-cadherin and subsequent cancer cell migration and invasion.

In the past decades, the roles of EMT-TFs have been re-evaluated; for example, it is suggested that EMT-TFs play pleiotropic roles beyond EMT during tumor development and progression (7). These transcription factors confer on cells the capacity for self-renewal, tumor initiation and survival in response to therapy, as well as facilitating immune evasion (5,6); however, the underlying molecular mechanisms remain unclear.

Immune evasion, one of the hallmarks of cancer progression (8,9), is often accomplished through expansion of an immune checkpoint signal, namely the programmed cell death 1 (PD-1)/PD-1 ligand (PD-L1; CD274) axis, or through recruitment of immunosuppressive cells such as tumor-associated macrophages (8,10). EMT correlates with tumor immune evasion and suppression within the tumor microenvironment (TME) (8). For example, tumors arising from mesenchymal

cancer cells exhibiting EMT markers facilitate formation of an immunosuppressive microenvironment to a greater extent than tumors derived from epithelial cancer cells (11). Within the TME, cancer cells with a mesenchymal phenotype are less susceptible than epithelial cancer cells to attack by CD8 T or natural killer cells and can induce immunosuppression via crosstalk with stromal immune cells (8). In addition, mesenchymal characteristics are associated with resistance to immune checkpoint inhibitors (ICIs) (12). EMT status correlates with levels of PD-L1 expression on tumor cells (13); however, the underlying molecular mechanisms are largely unknown and it is not yet clear whether immune suppression and evasion within the TME are promoted directly by EMT-TFs.

Previously, we reported that ZEB2 cooperates with SP1 to act as a transcriptional activator that mediates diverse cellular functions, including cancer cell survival, growth and angiogenesis, as well as EMT and invasion, all of which lead to metastasis (14-16). Therefore, it was hypothesized that by cooperating with SP1, ZEB2 in cancer cells may drive immune suppression and evasion during tumor progression. In particular, the present study aimed to determine whether cooperation between ZEB2 and SP1 modulates cytotoxic T cell activity and macrophage recruitment.

It was found that ZEB2 upregulated expression of PD-L1 and CCL2 through cooperation with SP1, thereby suppressing T cell activity and macrophage recruitment *in vitro*; in addition, ZEB2 suppressed the activity of tumor-infiltrating T cells in a syngeneic mouse tumor model. Clinically, *ZEB2* expression associated positively with expression of *CD274* and *CCL2* in human cancers. Furthermore, SUMOylation of ZEB2 was required for cooperation with SP1 and subsequent gene expression, a finding that provides a clue to understanding regulation of the ZEB2-SP1 cooperation event. Taken together, the data demonstrated the molecular mechanism underlying immune suppression mediated directly by an EMT-inducing transcription factor.

Materials and methods

Cell lines. Human embryonic kidney 293E (293E) cells (ATCC) were maintained at 37˚C/5% CO_2 in DMEM (HyClone; Cytiva) containing 10% fetal bovine serum (FBS; Thermo Fisher Scientific, Inc.). SW480 (colon cancer), PC3 (prostate cancer), Jurkat (acute T cell leukemia, T lymphoblast), THP-1 (acute monocytic leukemia, monocyte) (all from ATCC) and SNU-398 (liver cancer; Korean Cell Line Bank) cells were maintained in RPMI1640 (HyClone; Cytiva) containing 10% FBS. Stable cells (ZEB2-suppressed vs. control cells) were established from the SNU-398 cell lines as described previously (16). Hepa 1-6 (mouse liver cancer) cells (a kind gift from Laboratory Animal Resource Center, Ochang campus, Korea Research Institute of Bioscience and Biotechnology) were maintained in DMEM containing 10% FBS and Renca (mouse kidney cancer Korean Cell Line Bank) cells were maintained in Minimum Essential Medium containing 10% FBS, Non-Essential Amino Acids and sodium pyruvate. Cells were checked for mycoplasma contamination and their identities were confirmed using short tandem repeat (STR)-polymerase chain reaction (PCR).

Transfection with expression vectors and small interfering (si)RNA. Cells were transfected with a vector expressing ZEB2 (pCS3 SIP1; a kind gift from Dr D. Huylebroeck, University of Leuven, Belgium) at 37˚C using Lipofectamine® 2000 (Invitrogen; Thermo Fisher Scientific, Inc.) or electroporation (Invitrogen; Thermo Fisher Scientific, Inc.). Cells were transfected with 40 nM of siRNA specific for *ZEB2* (5'-CAACAUAUCCACUCCAUUU-3'), *SP1* (5'-GGUAGCUCUAAGUUUUGAU-3') or *CBX4* (PC2) (5'-AAGUACUACUACCAGCUCAAC-3') using Lipofectamine® 2000 (Invitrogen; Thermo Fisher Scientific, Inc.) at 37˚C for 48 h prior to analysis. A scrambled or non-targeting siRNA (5'-AUUAUCCACCUAAUACCUC-3' for *ZEB2*, 5'-GUUCAGCGUGUCCGGCGAG-3' for *SP1*, and 5'-ACAACACGGCUAAUCAACUCU-3' for *CBX4*) was used as a negative control. Where indicated, cells were co-transfected for 48 h with both siRNA and a plasmid (pCS3 SIP1; 2 μg per well of 6-well plates). Cells were transfected with the ZEB2 expression vector for 48 h and then treated with cycloheximide (100 μM; MilliporeSigma) or 0.1% dimethyl sulfoxide for up to 24 h.

The mutant ZEB2 (K391R/K866R double mutation) construct was generated using the EZchange site-directed mutagenesis kit (Enzynomics) and the following mutagenesis primers: K391R: 5'-AACAGAACCACTAGACTTCAATGACTATAAAGTTC-3' and 5'-CTAATCTTAAGTAAGCCTGTCTGCTCAGACATGCTA-3'; K866R: 5'-GACTTTTATCAGGAAAGAGTTTTC-3' and 5'-AAATTCAGAGGCTCATCTGAATTC-3' (the mutated nucleotide is underlined). *CBX4* siRNA 5'-AAGTACTACTACCAGCTCAAC-3' and scrambled control 5'-ACAACACGGCTAATCAACTCT-3' were subcloned into the pLKO.1 short hairpin (sh)RNA vector in accordance with the manufacturer's instructions (Addgene, Inc.). The SUMO1, SUMO2 and SUMO3 expression vectors were described previously (17). An siRNA specific for *Sp1* (5'-GGAUGGUUCUGGUCAAAUACA-3') and a scrambled siRNA (5'-GGGUGCAUAUACAGAUUGACU-3') were also used.

Immunoblot analysis. Whole-cell lysates were prepared using RIPA buffer (Biosolution Co., Ltd.,) and protein concentration was determined by Bradford method (Bio-Rad Protein Assay Dye Reagent Concentrate; Bio-Rad Laboratories, Inc.) and 20 μg of lysates were then subjected to immunoblotting as described previously (16) using the following primary antibodies: Anti-β-actin (cat. no. sc-47778), anti-SP1 (cat. no. sc-17824), anti-PC2 (cat. no. sc-517216), anti-VEGF (sc-152), and anti-GAPDH (cat. no. sc-32233; Santa Cruz Biotechnology, Inc.); anti-myc (cat. no. 05-724; Merck KGaA); anti-integrin α5 (cat. no. 610633; BD Biosciences); anti-flag (cat. no. F1804) and anti-vimentin (cat. no. V6389; MilliporeSigma); anti-PD-L1 (cat. no. 13684), anti-CCL2 (cat. no. 2027), anti-phosphorylated (p-)extracellular signal-regulated kinase 1/2 (ERK1/2) (cat. no. 9102), anti-ERK1/2 (cat. no. 9101), anti-p-AKT (S473) (cat. no. 4051), anti-AKT (cat. no. 7272), anti-survivin cat. no. (2803), anti-cyclin D1 (cat. no. 2978), anti-BCL-2 (cat. no. 2870), anti-SNAIL (cat. no. 3879), anti-PARP (cat. no. 9542) and anti-myc (cat. no. 2272; Cell Signaling Technology, Inc.); anti-ZEB2 (6E5; cat. no. 61095, Active Motif, Inc.); and anti-E-cadherin (cat. no. MAB1838; R&D Systems). Briefly, lysates were loaded onto 6-12%

polyacrylamide gels and proteins were transferred to PVDF membrane (Bio-Rad Laboratories, Inc.). The membranes were blocked with 5% skimmed milk for 1 h at room temperature, incubated with primary antibody (1:1,000 dilution) for 16 h at 4˚C, and then incubated with secondary antibody [goat anti-rabbit IgG conjugated with horseradish peroxidase (1:10,000 dilution, cat. no. 1706515; Bio-Rad Laboratories, Inc.) or goat anti-mouse IgG conjugated with peroxidase (1:5,000 diluted, cat. no. 401215; MilliporeSigma)] for 1 h at room temperature. Chemiluminescent substrates solution (Claro Sola ECL solution; BioD Co., Ltd.) was used to visualize the signal. Densitometric quantification was performed with ImageJ v1.52p (National Institutes of Health). RIPA buffer containing 20 mM N-ethylmaleimide (NEM; deSUMOylation inhibitor) was used to prepare lysates prior to detection of protein SUMOylation. Subcellular fractions were prepared using the Compartmental Protein Extraction Kit (MilliporeSigma).

Reverse transcription-quantitative (RT-q) PCR. Total RNA was isolated using TRIzol® (Invitrogen; Thermo Fisher Scientific, Inc.) from cells at density of ~80% and cDNA was synthesized using reverse transcriptase (Bioneer Corporation) according to the manufacturer's protocols. qPCR was performed in 20 μl reaction volume using an SYBR Green qPCR Master Mix (PKT; https://philekorea.kr), a Rotor-Gene 6000 real-time rotary analyzer (Corbett) and primers (forward and reverse, respectively) specific for *ZEB2* (5'-TTGAGGAGA CTGCCCAATAA-3' and 5'-TATATCCAGGGCCCTACA GC-3'), *CCL28* (5'-AAGGAAATGTTTGCCACAGG-3' and 5'-ATGGCCGTATGTTTCGTGTT-3'), *CXCL2* (5'-CACACT CAAGAATGGGCAGA-3' and 5'-GCTTCCTCCTTCCTT CTGGT-3'), *CXCL3* (5'-GTCCCTGCCCTTACCAGAG-3' and 5'-GTCAAACACATTAAGTCCTTTCCA-3'), *CXCL6* (5'-CGCTGAGAGTAAACCCCAAA-3' and 5'-AACTTGCTT CCCGTTCTTCA-3'), *CXCL12* (5'-GTGGTCGTGCTGGTC CTC-3' and 5'-GCTCTGGCAACATGGCTTT-3'), or *GAPDH* (5'-CATGACCACAGTCCATGCCAT-3' and 5'-AAGGCC ATGCCAGTGAGCTTC-3').

The following specific primers (forward and reverse, respectively) were used to target M1 and M2-type markers: *TNF* (5'-TGAAAGCATGATCCGGGACG-3' and 5'-CAA AGTGCAGCAGGCAGAAG-3'); *CXCL8*/*IL8* (5'-TCTGTG TGAAGGTGCAGTTTT-3' and 5'-GGGGTGGAAAGGTTT GGAGTA-3'); *IL12B* (5'-CTGAAGAAGATGGTATCACCT GGAC-3' and 5'-TTAGAACCTCGCCTCCTTTGTG-3'); *NOS2*/*INOS* (5'-GAGCCAGGCCACCTCTATGT-3' and 5'-GTCCTCGACCTGCTCCTCAT-3'); *IL1B* (5'-GTACCT GTCCTGCGTGTTGA-3' and 5'-GGGAACTGGGCAGAC TCAAA-3'); *IL6* (5'-CCAGAGCTGTGCAGATGAGT-3' and 5'-AGTTGTCATGTCCTGCAGCC-3'); *IL10* (5'-GGCGCT GTCATCGATTTCTT-3' and 5'-ATAGAGTCGCCACCCTGA TG-3'); *TGFB1* (5'-AAGGACCTCGGCTGGAAGTGC-3' and 5'-CCGGGTTATGCTGGTT-3'); *MRC1* (5'-GCAGTCCTT TCCGATATTTGA-3' and 5'-CCCAGTTTCTGAACACAT TCC-3'); *CLEC10A* (5'-AGAATAAGGTGAAAGTCCAGG GG-3' and 5'-GCTAAAATCTGTTCTCAGGGTCAC-3'); *CCL17* (5'-CCTTAGAAAGCTGAAGACGTGGTA-3' and 5'-TCTTCACTCTCTTGTTGTTGGGG-3'); and *ARG1* (5'-TCATCTGGGTGGATGCTCACAC-3' and 5'-GAGAAT CCTGGCACATCGGGAA-3'). PCR steps of denaturation (95˚C; 15 sec), annealing (60˚C; 15 sec) and extension (72˚C; 15 sec) were repeated for 40 cycles.

qPCR was performed using QuantiTect Probe PCR Master Mix (Qiagen GmbH) and primers (forward and reverse, respectively) and probes specific for *CD274* (5'-ATGTGACCA GCACACTGAGA-3', 5'-TCAGTGCTACACCAAGGCAT-3' and FAM 5'-TGGTCATCCCAGAACTACCTCTGGCA-3' TAMRA) or *CCL2* (5'-GCTCAGCCAGATGCAATCAA-3', 5'-ACAGATCTCCTTGGCCACAA-3' and FAM 5'-AGCTCG CGAGCCTCTGCACT-3' TAMRA). PCR steps of denaturation (94˚C; 15 sec) and combined annealing/extension (60˚C; 60 sec) were repeated for 45 cycles, according to the manufacturer's protocol.

Quantification of all qPCR was performed according to the Rotor-Gene® Q User Manual (Qiagen GmbH). All determinations were performed in three independent experiments.

Promoter reporter assay. Cells were transfected with Lipofectamine® 2000 (Invitrogen; Thermo Fisher Scientific, Inc.). Briefly, $2x10^5$ cells were seeded onto 6-well plates and incubated for 24 h. Next, cells were co-transfected with 2 μg of reporter plasmid DNA and 1.8 μg of the ZEB2 expression vector. At 48 h post-transfection, firefly luciferase activity was measured in a Dual-luciferase reporter assay system (Promega Corporation). Transfection efficiency was normalized by measuring *Renilla* luciferase activity encoded by the co-transfected *Renilla* luciferase vector (pRL-TK). For siRNA transfection, cells were transfected for 24 h with siRNA, followed by transfection with reporter plasmids.

The *ITGA5* (integrin α5) promoter (-908/+241), the *CDH1* (E-cadherin) promoter (-308/+41), the *VIM* (vimentin) promoter (-411/+60) and the *VEGF* promoter (-2361/+298) constructs, as well as the SP1 cis-element reporter plasmid (TATA-SP1 reporter), were described previously (14,16). Briefly, the *ITGA5* promoter was obtained by PCR with primer set (forward 5'-CCGCTCGAGGAGCTGAAGGTT GGGTCC-3' and reverse 5'-CCGCTCGAGCCGTCTGTT CCCGGC-3') using genomic DNA from SW480 cells and then the PCR product was subcloned into the pGL3 basic vector (Promega Corporation). The *CDH1* promoter construct was kindly provided by Dr G. Berx (V.I.B.-Ghent University, Belgium). The *VIM* promoter construct was kindly provided by Dr S. Rittling (The Forsyth Institute, MA, USA). The *VEGF* promoter construct was kindly provided by Dr S.G. Chi (Korea University, Korea). The TATA-SP1 reporter was a kind gift from Dr Yann Leverrier (Inserm, France). The human *CD274* (PD-L1) promoter (-3153/+1) reporter was generated from the *CD274* promoter (-3153/-82) construct (purchased from Addgene; cat. no. 107004) by inserting the sequence 5'-GTG GGCGGGACCCCGCCTCCGGGCCTGGCGCAACGCTGA GCAGCTGGCGCGTCCCGCGCGGCCCCAGTTCTGCGC AGCTTCC-3' (the SP1 site is underlined). The *CCL2* promoter (-2855/+60) reporter was a kind gift from Dr Srinivas Mummidi (University of Texas Health Science Center, TX, USA) (18). The mutant *CD274* promoter and the *CCL2* promoter reporter constructs (ΔSp1) were generated using the QuikChange site-directed mutagenesis kit (Agilent Technologies, Inc.) and the following primers: *CD274* promoter 5'-CTGCCTTGGGCA GAGGTGGATAGGACCCCGCCT-3' and its complementary

strand; and *CCL2* promoter 5'-CTCCTCCTGCTTGAC TCATACCTCTCTCCCTCTGCCC-3' and its complementary strand (the mutated nucleotides are underlined).

Chromatin immunoprecipitation (ChIP). ChIP assays were performed in accordance with the instructions supplied with the Pierce Magnetic ChIP Kit (cat. no. 26157; Thermo Fisher Scientific, Inc.). Briefly, the equivalent of $1x10^6$ SNU-398 cells was used for each ChIP reaction with 2 μg of anti-SP1 (E-3; Santa Cruz Biotechnology, Inc.) and anti-ZEB2 (H260; Santa Cruz Biotechnology, Inc.) antibodies for 16 h at 4˚C. Normal mouse IgG was used as the control. Immunoprecipitated and input (1%) DNAs were analyzed by semiquantitative PCR using *CD274* promoter-specific primers (5'-ACACCAACACTAGAT ACC-3' and 5'-CTCAGCGTTGCGCCAGGC-3' for -181/-41 and 5'-TCTGTCATCTTGGGCCCA-3' and 5'-CCATCCCGA GCTACATCTT-3' for -807/-660) and *CCL2* promoter-specific primers (5'-GATTTAACAGCCCACTTATC-3' and 5'-TGG ATGTTTCTGGGTTAG-3' for -115/+25 and 5'-GCAGGG CTCGAGTTGATT-3' and 5'-TTCCTGGGACTAGACTTG-3' for -1820/-1675). Briefly, PCR was performed using Taq DNA polymerase (cat. no. HS106; BioFACT). PCR steps of denaturation (95˚C; 20 sec), annealing (58˚C; 30 sec) and extension (72˚C; 20 sec) were repeated for 35 cycles and final extension step at 72˚C was maintained for 5 min. PCR products were loaded onto 2% agarose gel and visualized/quantified by Image Lab Software v3 (Bio-Rad Laboratories, Inc.) on the Gel Doc XR+ System (Bio-Rad Laboratories, Inc.).

Nuclear factor of activated T cells (NFAT) activity assay. Jurkat cells were transfected for 24 h at 37˚C with an NFAT-reporter construct [pGL4.30(*luc2P*/NFAT-RE/Hygro); Promega Corporation] using Lipofectamine®. Stable SNU-398 cells ($2.5x10^4$ cells/well) were seeded onto 96-well plates for 24 h. Next, transfected Jurkat cells were harvested and replated into the 96-well plates containing SNU-398 cells ($2x10^4$ cells/well). At 24 h after replating, Jurkat cells were treated with phorbol 12-myristate 13-acetate (PMA; 50 ng/ml) and ionomycin (1 μM) for 24 h. At 72 h after transfection, luciferase activity (which represents NFAT activity) was measured in a Bright-Glo Luciferase Assay System (Promega Corporation). Where indicated, an anti-PD-1 antibody (Pembrolizumab; Merck KGaA) was added.

Analysis of secreted CCL2 and IL-2 in an enzyme-linked immunosorbent assay (ELISA). The amount of CCL2 protein in conditioned medium from cells was measured using a Human CCL2 Quantikine ELISA kit (cat. no. DCP00; R&D Systems). The amount of IL-2 secreted from Jurkat cells co-cultured with stable SNU-398 cells was measured using a Human IL-2 uncoated ELISA kit (cat. no. 88-7025-88; Invitrogen; Thermo Fisher Scientific, Inc.).

Flow cytometry. To analyze expression of PD-L1 on the cell surface, SW480 cells were transfected for 48 h at 37˚C with ZEB2, SNAIL, TWIST1 (19), or PD-L1 (Addgene cat. no. 124686) expression vectors prior to staining with an APC-conjugated anti-PD-L1 antibody (cat. no. 329708; BioLegend, Inc.). Viable propidium iodide-negative cells were analyzed by flow cytometry. SW480 cells, incubated for 48 h at 37˚C with interferon (IFN)-γ (10 ng/ml), were used as a positive control.

Cell survival analysis. Survival of cells in suspension culture was determined. Briefly, cells were seeded into 96-well plates ($3x10^4$ cells/well) with an Ultra-Low Attachment Surface (Corning, Inc.) and then incubated for 3 days at 37˚C in the absence of serum. Cell viability was measured in a colorimetric WST assay (16).

Cell migration and invasion assays. THP-1 cell suspensions ($1x10^4$) were seeded to 8-μm pore Transwell inserts (Corning, Inc.) in the presence of PMA (10 ng/ml) for 24 h and then washed with serum-free medium. The Transwell inserts were then moved to 24-well plates containing concentrated conditioned medium from stable SNU-398 cells, VEGF (20 or 100 ng/ml), CCL2 (10 or 50 ng/ml), or pre-seeded stable SNU-398 cells ($1x10^5$). The cells were allowed to migrate for 24 h. Where indicated, an anti-CCL2 antibody (5 μg/ml; MAB679, R&D systems) was added to block the activity of CCL2. Inserts were fixed with 10% formalin for 16 h at 4˚C and stained with 2% crystal violet for 1 h at room temperature. The number of cells that had migrated was counted in five representative (x100) fields per insert using light microscope. An invasion assay using SW480 cells transfected with ZEB2 was performed as described previously (16). Briefly, cells were plated in serum-free medium on Transwell inserts coated with 25 μg of Matrigel (BD Biosciences). The underside of the insert was pre-coated with 2 μg of collagen type I (MilliporeSigma). After incubation for 48 h at 37˚C, inserts were fixed and stained. The number of cells that had invaded was counted as described above.

Anchorage-independent growth assay (soft agar assay). Cells in 0.3% agar were seeded into 6-well tissue culture plates ($3x10^3$ cells/well) over a 0.6% agar feed layer and then allowed to grow at 37˚C/5% CO_2 for 21 days. The number of colonies (>30 μm in diameter) in each well was then counted.

Co-immunoprecipitation. 293E cells were co-transfected with a vector expressing myc-tagged ZEB2 (WT or K391/866R mutant; backbone plasmid was pCS3 SIP1) and an SP1 (a kind gift from Dr G. Suske, Philipps-Universitat Marburg, Germany) expression vector for 48 h at 37˚C using Lipofectamine® 2000 (Invitrogen; Thermo Fisher Scientific, Inc.). Then, cells were lysed with co-immunoprecipitation buffer [10 mM HEPES (pH8.0), 150 mM NaCl, 0.1 mM EDTA, 20% glycerol, 0.2% NP-40] supplemented with a protease inhibitor (Complete; Roche Diagnostics). Lysates were centrifuged for 20 min at 10,000 x g at 4˚C and the supernatant (2 mg of lysates for each immunoprecipitation reaction) was precleared for 2 h at 4˚C by incubation with TrueBlot Anti-Mouse Ig IP beads (cat. no. 00-8811-25, Rockland Immunochemicals, Inc.). The precleared supernatant was immunoprecipitated for 16 h at 4˚C with 1 μg of anti-myc or anti-SP1 antibodies and the protein complexes were collected by incubation with TrueBlot Anti-Mouse Ig IP beads for 2 h at 4˚C. The complexes were then washed three times with co-immunoprecipitation buffer and centrifugation for 2 min at 1,200 x g at 4˚C. After last centrifugation, supernatant was removed and complexes were

eluted by boiling in SDS sample buffer. Finally, proteins were analyzed by immunoblotting with anti-myc and anti-SP1 antibodies.

Generation of stable cell lines. To generate lentiviruses, Lenti-X-293T cells (Clontech) were co-transfected with the pLKO.1 shRNA construct (*Zeb2* siRNA 5'-CATCAGACTTTG AGGAATA-3' and scrambled control 5'-ATTATCCACCTA ATACCTC-3') and a Lentiviral Packaging Mix (Sigma) using Lipofectamine® 2000 (Invitrogen; Thermo Fisher Scientific, Inc.) for 48 h at 37˚C. Next, Hepa1-6 cells were transduced for 12 h with concentrated lentiviruses in the presence of polybrene (4 μg/ml) and then selected for 2 weeks with puromycin (1 μg/ml) to establish stable clones.

In vivo syngeneic mouse tumor model. All animal procedures were performed in accordance with the guidelines of the Animal Care Committee at the Korea Research Institute of Bioscience and Biotechnology (KRIBB) and were approved by the bioethics committee of KRIBB (approval nos. KRIBB-AEC-22107 and KRIBB-AEC-23130). C57BL/6 mice (5-week-old female; n=10; body weight 16-18 g) were purchased from Koatech. Mice were housed under a 12 h light/dark cycle, with lights from 7:00 a.m. -7:00 p.m. The temperature was maintained at 22±2˚C, and the relative humidity was kept between 45 and 55%. Hepa1-6 stable cells (Zeb2-suppressed and control cells) were injected subcutaneously into the flank of each mouse ($1x10^7$ cells per mouse; n=5 per group). Tumor volume (0.5 x length x width x height) and body weight were measured twice per week. On day 35, mice were euthanized by CO_2 gas inhalation (CO_2 fill rate was ~50% of the chamber volume per min). The mice were left for at ≥3 min after respiratory arrest and were observed carefully to ensure cessation of breathing and heartbeat. Only then was cervical dislocation performed. Tumors were excised and divided into two parts: one was used for flow cytometry analysis and the other for RNA extraction.

Preparation of single-cell suspensions and antibody staining for flow cytometry. Mouse tumors were dissociated into single-cell suspensions using a Tumor Dissociation Kit and gentleMACS Octo Dissociator with Heaters (Miltenyi Biotec GmbH). Dissociated tumors were washed twice in PBS and filtered through 70- and 40-μm cell strainers. Red blood cells were lysed and debris removed to obtain single-cell suspensions. To detect intracellular cytokines, cells were resuspended in complete RPMI1640 (containing 10% FBS and antibiotics) and then stimulated at 37˚C for 3.5 h with 50 ng/ml PMA and 1 μM ionomycin in the presence of GolgiStop (BD Biosciences). The cells were then blocked with anti-mouse CD16/CD32 and stained at 4˚C for 30 min with anti-CD45 (FITC; BD Biosciences), anti-CD3 (APC-Cy7; BD Biosciences), anti-CD4 (BV 510; BioLegend), or anti-CD8 (PE; BD Biosciences) antibodies. The cells were then fixed and permeabilized using a Cytofix/Cytoperm Kit (BD Biosciences) prior to staining at 4˚C for 30 min with an anti-IFN-γ antibody (PE-Cy7; BD Biosciences). To detect macrophages, single cells were blocked with anti-mouse CD16/32 and stained at 4˚C for 30 min using anti-CD45 (FITC; BD Biosciences), anti-F4/80 (PerCP; BioLegend) and anti-CD11b (APC; BD Biosciences) antibodies. Events were acquired by a BD FACSAria III (BD Biosciences) instrument and data were analyzed by FlowJo software version 10 (FlowJo LLC).

Whole tumor RNA extraction and RT-qPCR. Total RNA was extracted from syngeneic mouse tumors using TRIzol® (Invitrogen) and cDNA was synthesized using reverse transcriptase (Bioneer Corporation) according to the manufacturer's protocols. qPCR was performed using SYBR Green qPCR Master Mix (PKT), Rotor-Gene 6000 real-time rotary analyzer (Corbett) and primers (forward and reverse, respectively) specific for *Zeb2* (5'-TCGAGAGGCATATGG TGACG-3' and 5'-TACCTGCTCCTTGGGTTAGC-3'), *Tnf* (5'-CCCTCACACTCAGATCATCTTCT-3' and 5'-GCT ACGACGTGGGCTACAG-3'), *Ifng* (5'-GCTTTGCAGCTC TTCCTCAT-3' and 5'-CCAGTTCCTCCAGATATCCAA G-3'), *Il2* (5'-GGACCTCTGCGGCATGTTCT-3' and 5'-ACA GTTGCTGACTCATCATCGAATT-3'), *Il10* (5'-TGAAGA CCCTCAGGATGCGG-3' and 5'-AGAGCTCTGTCTAGG TCCTGG-3'), or *GAPDH* (5'-CCAATGTGTCCGTCGTGG AT-3' and 5'-TGGTCCTCAGTGTAGCCCAA-3'). PCR steps of denaturation (95˚C; 15 sec), annealing (60˚C; 20 sec), and extension (72˚C; 20 sec) were repeated for 40 cycles. Quantification was performed according to the Rotor-Gene® Q User Manual (Qiagen GmbH). qPCR determinations were performed in three independent experiments.

mRNA-seq analysis. Total RNA was extracted from SW480 (ZEB2-overexpressing and control) cells, followed by mRNA-Seq analysis by commercial service (Macrogen, Inc.). Based on differential expression of genes, Kyoto Encyclopedia of Genes and Genomes (KEGG) pathways were analyzed by commercial service (Macrogen, Inc.). Briefly, differentially expressed genes were selected by |fold change|≥2 and P-value <0.05. To explore significantly enriched functions, KEGG pathway analysis was performed using KEGG Viewer script (Macrogen, Inc.) against KEGG pathway database (http://www.genome.jp/kegg/pathway.html). Adjusted P-values reported from KEGG viewer result were derived using two-sided modified Fisher's exact test and corrected by Benjamini-Hochberg method.

Analysis of The Cancer Genome Atlas (TCGA) and Gene Expression Omnibus (GEO) datasets. cBioPortal (www.cbioportal.org) (20,21) was used to analyze TCGA-generated human colorectal adenocarcinoma data [four cancer studies: TCGA, Nature 2012 (22); TCGA, Firehose Legacy; CPTAC-2, Prospective, Cell 2019 (23); and TCGA, PanCancer Atlas] and pancreatic adenocarcinoma data (TCGA Firehose Legacy). All patient samples for which mRNA expression profiles were available were included in analysis of each cancer study. Spearman's correlation coefficient (ρ) and the P-value were calculated using the cBioPortal webpage. Survival curve analysis was performed using the cBioPortal webpage tools. Raw datasets were downloaded from GEO (GSE62232 and GSE35896). Gene expression profiles derived from DNA microarray datasets were analyzed using BRB-Array Tools (24). GEPIA (gepia.cancer-pku.cn) was used to analyze 33 TCGA and Genotype-Tissue Expression (GTEx) datasets. Both TCGA normal and GTEx data were selected as matched

normal data for analysis of *CBX4* mRNA level (tumor vs. normal).

Statistical analysis. Statistical analyses were performed using unpaired Student's t-test, one-way ANOVA with Dunnett's or Tukey's multiple comparison post-test [with GraphPad Prism 8 (Dotmatics)], the log-rank test (for survival analysis) and Spearman's test (for correlation analysis). P<0.05 was considered to indicate a statistically significant difference.

Results

ZEB2 upregulates expression of PD-L1 and CCL2. First, the present study considered whether ZEB2 regulated expression of immunoregulatory factors involved in modulating the TME. Analysis of hepatocellular carcinoma (GSE62232) and colorectal cancer (GSE35896) datasets revealed that *ZEB2* expression correlated markedly with expression of cytokines (including *CCL2*, *CXCL12*, *TGFβ1*, *CCL11* and *CCL21*) and *CD274* (Fig. S1A and B).

Next, the present study performed mRNA sequencing analysis to determine the effect of ZEB2 on gene expression in ZEB2-overexpressing SW480 cells and control cells. Analysis of KEGG pathways revealed that ZEB2 expression correlated markedly with 'cytokine-cytokine receptor interactions', 'pathways in cancer', 'chemokine signaling pathways' and others (Fig. 1A, upper). Expression of cytokine-related genes (Fig. 1A, lower) and *CD274* (by 1.44-fold; P=0.01742) was higher in ZEB2-overexpressing cells than in control cells (Fig. 1A). RT-qPCR showed that *ZEB2* expression in ZEB2-overexpressing SW480 and/or ZEB2-suppressed SNU-398 cells correlated with expression of *CCL2*, *CCL28*, *CXCL2*, *CXCL3*, *CXCL6*, *CXCL12 and CD274* (Fig. 1B and C). Immunoblot analysis showed that overexpression of ZEB2 in SW480 cells upregulated CCL2 and PD-L1 and that suppression of ZEB2 in SNU-398 cells reduced expression of CCL2 and PD-L1 (Fig. 1D). Similarly, in PC3 cells, ZEB2 upregulated expression of PD-L1 and CCL2 at both the mRNA (Fig. S2A) and protein (Fig. 1D) levels.

Reporter assays using the *CD274* promoter (-3153/+1) and *CCL2* promoter (-2855/+60) revealed that ZEB2 enhanced the promoter activity of *CD274* and *CCL2* in SW480 cells, but suppression of ZEB2 reduced the promoter activity of *CD274* and *CCL2* markedly in SNU-398 cells (Fig. 1E). TWIST1 increased the promoter reporter activity of *CD274* and *CCL2*, while SNAIL moderately reduced and enhanced the promoter reporter activity of *CD274* and *CCL2*, respectively, in SW480 cells (Fig. S2B). Flow cytometry analysis showed that ZEB2 upregulated PD-L1 expression on the SW480 cell surface substantially (Fig. 1F). An ELISA revealed that secretion of CCL2 by SNU-398 cells was reduced markedly upon suppression of ZEB2 (Fig. 1G).

Analysis of TCGA-generated colorectal adenocarcinoma [two cancer studies: TCGA, Firehose Legacy and TCGA, Nature 2012 (22)] revealed that *ZEB2* expression correlated markedly with that of *CD274* (n=382, ρ=0.588, P=7.00e-37; and n=244, ρ=0.55, P=9.82e-21, respectively) and *CCL2* (ρ=0.823, P=1.43e-95; and ρ=0.707, P=2.96e-38, respectively; Fig. 1H and I). The TCGA Firehose Legacy study showed that *TWIST1* expression correlated with expression of *CD274* (ρ=0.373, P=4.60e-14) and *CCL2* (ρ=0.652, P=1.20e-47) and *SNAI1* expression correlated with expression of *CD274* (ρ=0.281, P=2.23e-08) and *CCL2* (ρ=0.508, P=1.73e-26; Fig. S1C) and the correlation was weaker than that for *ZEB2*.

Similarly, analysis of pancreatic adenocarcinoma (TCGA, Firehose Legacy study) showed that *ZEB2* expression correlated markedly with that of *CD274* (n=179, ρ=0.597, P=1.18e-18) and CCL2 (ρ=0.426, P=2.78e-9); however, expression of *TWIST1* did not correlate markedly with that of *CD274* (ρ=0.115, P=0.125) or *CCL2* (ρ=0.0682, P=0.365). Expression of *SNAI1* correlated markedly with that of *CD274* (ρ=0.296, P=5.675e-5) and *CCL2* (ρ=0.615, P=4.94e-20) (Fig. S1D).

The present study also found that low expression of both *ZEB2* and *CD274* in pancreatic adenocarcinoma (TCGA, Firehose Legacy) and colon cancer [CPTAC-2, Prospective, Cell 2019 (23)] patients correlated markedly with increased overall survival (Fig. 1J).

ZEB2 in cooperation with SP1 acts as a transcriptional activator of CD274 and CCL2. Next, the present study asked whether SP1 was involved in ZEB2-mediated expression of PD-L1 and CCL2. Suppression of SP1 led to a significant reduction in ZEB2-mediated expression of PD-L1 and CCL2 in SW480 cells at both the mRNA and protein levels (Fig. 2A and B). A reporter assay showed that deleting the -82/+1 region containing the consensus binding site for SP1 reduced ZEB2-induced *CD274* promoter activity in SW480 cells (Fig. S2C). The present study also analyzed functional involvement of the SP1 site using mutated *CD274* and *CCL2* promoter constructs. Mutation of the proximal SP1 site (-82/-70 for *CD274* and -67/-58 for *CCL2*) resulted in a substantial decrease in ZEB2-mediated activation of the *CD274* and *CCL2* promoters in SW480 cells (Fig. 2C). These observations indicated that ZEB2 upregulated PD-L1 and CCL2 in an SP1-dependent manner. Furthermore, the present study performed ChIP experiments to examine the interaction of ZEB2 and SP1 with the promoters of *CD274* and *CCL2* in SNU-398 cells, which expressed endogenous ZEB2. Chromatin fragments containing the *CD274* promoter (-181/-41) were pulled down specifically by anti-ZEB2 and anti-SP1 antibodies; however, an irrelevant region (-807/-660) was not pulled down efficiently (Fig. 2D). Similarly, chromatin fragments containing the *CCL2* promoter (-115/+25) were pulled down specifically by anti-ZEB2 and anti-SP1 antibodies, but an irrelevant region (-1820/-1675) was not (Fig. 2D). Taken together, these results suggested that ZEB2 cooperated with SP1 to upregulate transcription of *CD274* and *CCL2* by binding directly to their promoters.

ZEB2 suppresses T cell activation by upregulating PD-L1. Next, the present study investigated whether ZEB2-induced PD-L1 expression modulated T cell activity. Jurkat cells (human T lymphocytes) transiently transfected with a NFAT reporter construct were co-cultured for 48 h with ZEB2-suppressed stable SNU-398 cells or control cells (direct co-culture system). In subsequent reporter assays, treatment of Jurkat cells with PMA and ionomycin increased NFAT activity; however, NFAT activity in Jurkat cells decreased to a much greater extent upon co-culture with control SNU-398 cells than upon co-culture with ZEB2-suppressed

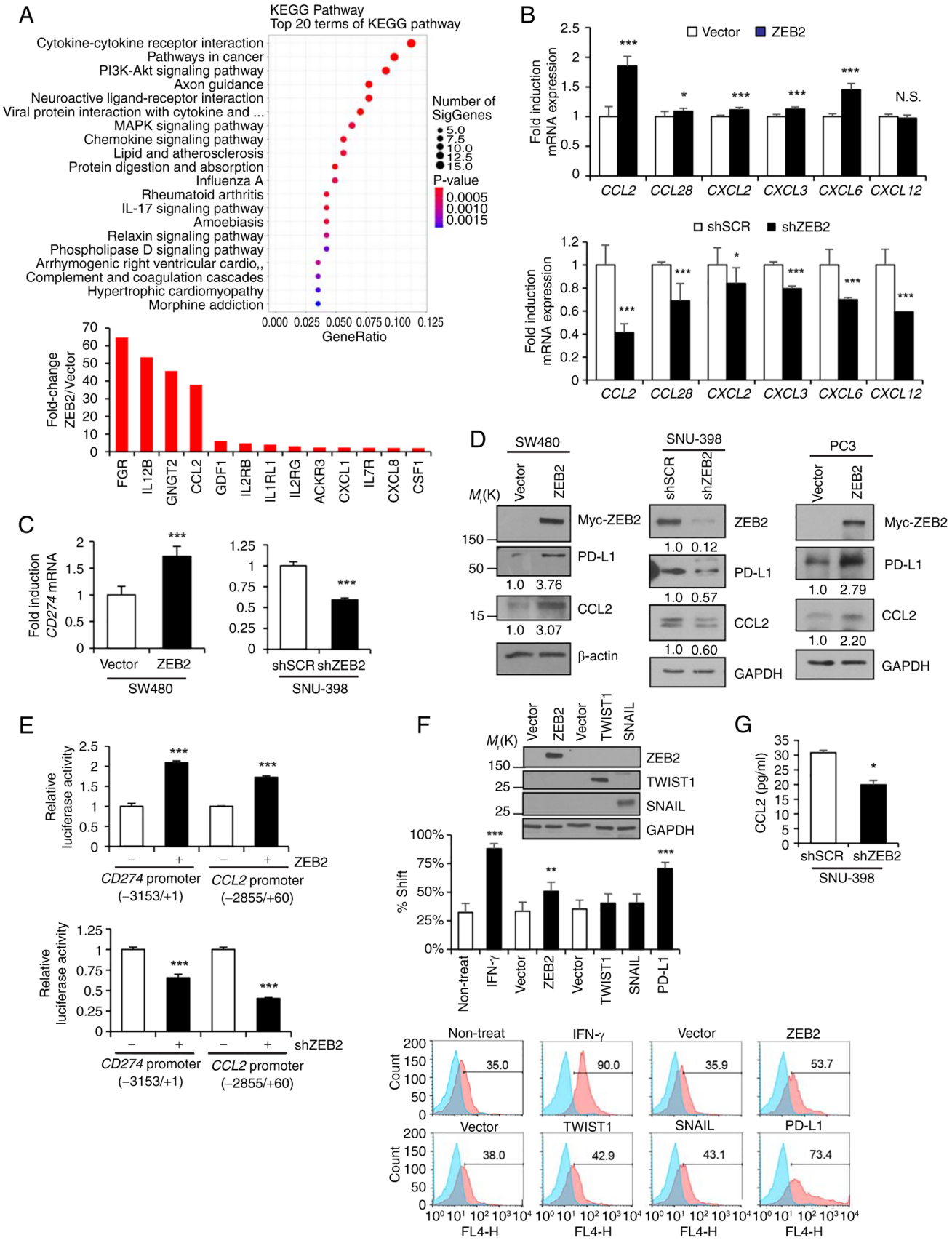

Figure 1. Continued.

cells (Fig. 3A). Consistent with this, the results of an ELISA showed that secretion of IL-2 by Jurkat cells decreased upon co-culture with control SNU-398 cells to a much greater extent than upon co-culture with ZEB2-suppressed cells (Fig. 3B). Immunoblot analysis showed that treatment of cells with PMA and ionomycin increased phosphorylation of

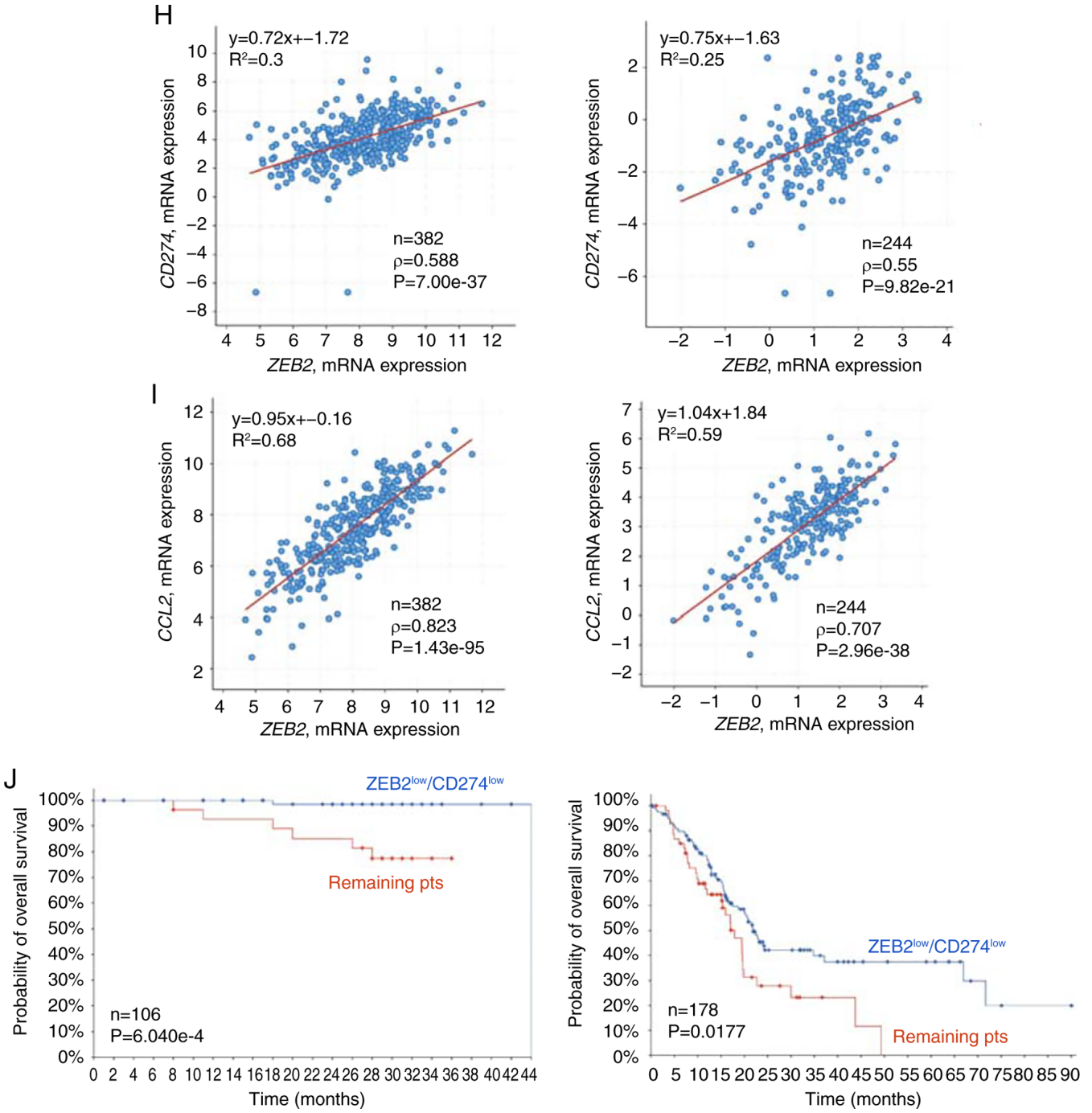

Figure 1. ZEB2 upregulates expression of PD-L1 and CCL2. (A) mRNA-seq analysis of ZEB2-overexpressing SW480 cells and analysis of KEGG pathways affected by ZEB2 expression. The size of each circle represents the number of genes involved in the corresponding pathway and the color scale denotes the P-value (upper). Changes in expression of cytokine-related genes in ZEB2-overexpressing SW480 cells are vs. those in control cells (lower). (B) RT-qPCR of *CCL2*, *CCL28*, *CXCL2*, *CXCL3*, *CXCL6* and *CXCL12* levels in ZEB2-overexpressing vs. control SW480 cells (upper) and in ZEB2-suppressed vs. control SNU-398 cells (lower; n=4). (C) RT-qPCR of *CD274* mRNA levels in ZEB2-overexpressing vs. control SW480 cells (left) and in ZEB2-suppressed vs. control SNU-398 cells (right; n=4). (D) Analysis of CCL2 and PD-L1 protein levels in ZEB2-overexpressing vs. control SW480 cells (left), in ZEB2-suppressed vs. control SNU-398 cells (middle) and in ZEB2-overexpressing vs. control PC3 cells (right). Densitometric quantification of bands on the immunoblot was performed, with β-actin or GAPDH as a loading control. (E) Reporter analysis of *CD274* and *CCL2* promoter activity in ZEB2-overexpressing vs. control SW480 cells (upper) and in ZEB2-suppressed vs. control SNU-398 cells (lower; n=4). (F) Flow cytometry analysis of PD-L1 expression in SW480 cells transfected with ZEB2, TWIST1, or SNAIL expression vectors (n=3). Cells treated with IFN-γ or transfected with a PD-L1 expression vector were used as positive controls. Immunoblot analysis confirmed overexpression of ZEB2 (anti-myc), TWIST1 (anti-flag) and SNAIL (anti-SNAIL). (G) ELISA to measure secreted levels of CCL2 in conditioned medium from ZEB2-suppressed vs. control SNU-398 cells (n=3). (H, I) Scatter plots of *ZEB2* mRNA expression vs. *CD274* (H) and *CCL2* (I) mRNA expression in colorectal adenocarcinoma (data from TCGA, Firehose Legacy and TCGA, Nature 2012). Correlations were statistically analyzed using the Spearman test. Spearman's correlation coefficients and equations were automatically generated using the cBioPortal webpage tool. (J) Kaplan-Meier analysis showing the relationship between overall survival of colon cancer (CPTAC-2, Prospective, Cell 2019; n=106) and pancreatic adenocarcinoma (TCGA, Firehose Legacy; n=178) patients and expression of *ZEB2* and *CD274* mRNA. P-values were calculated by the log-rank test. Values represent the mean ± standard deviation. *P<0.05; **P<0.01; ***P<0.001; N.S, not significant. ZEB2, Zinc Finger E-Box Binding Homeobox 2; PD-L1, programmed cell death 1 ligand 1; CCL2, C-C motif chemokine ligand 2; KEGG, Kyoto Encyclopedia of Genes and Genomes; RT-qPCR, reverse transcription-quantitative PCR; ELISA, enzyme-linked immunosorbent assay; TCGA, The Cancer Genome Atlas; sh, short hairpin.

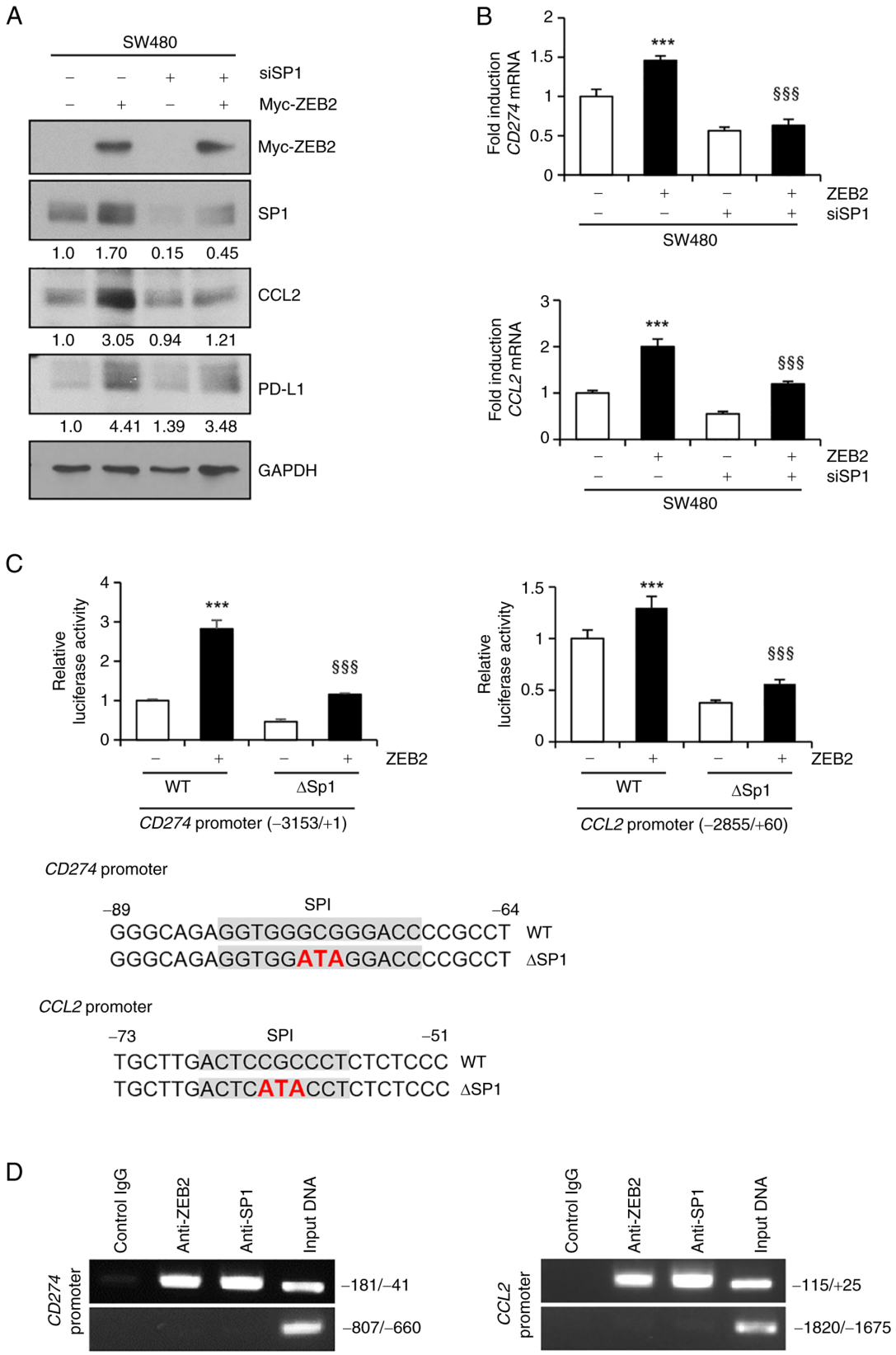

Figure 2. ZEB2 cooperates with SP1 to promote transcription of *CD274* and *CCL2* by binding directly to their promoters. (A) SW480 cells were co-transfected with siRNA specific for *SP1* (siSP1) and with a ZEB2 expression vector, for 48 h prior to immunoblot analysis. Densitometric quantification of bands on the immunoblot was performed, with GAPDH as a loading control. (B) RT-qPCR of *CD274* (upper) and *CCL2* (lower) levels in SW480 cells co-transfected with siSP1 and the ZEB2 expression vector (n=4). (C) Mutation analysis of the SP1 site in the *CD274* and *CCL2* promoters. SW480 cells were transfected with reporter constructs containing SP1 site mutations and reporter activity was measured (n=4). Values represent mean ± SD. ***P<0.001, vs. vector + control siRNA; §§§P<0.001, vs. ZEB2 + control siRNA. (D) ChIP analysis of the interaction between ZEB2 and SP1 and the *CD274* and *CCL2* promoters. Chromatin fragments from SNU-398 cells were immunoprecipitated by normal mouse IgG (lane 1), anti-ZEB2 (lane 2), or anti-SP1 (lane 3) and data were analyzed by semiquantitative PCR using *CD274* (-181/-41) and *CCL2* (-115/+25) promoter primers. The input control (1%) is shown in lane 4. Irrelevant regions (-807/-660 for *CD274* and -1820/-1675 for *CCL2*) were also analyzed. ZEB2, Zinc Finger E-Box Binding Homeobox 2; si, small interfering; RT-qPCR, reverse transcription-quantitative PCR; PD-L1, programmed cell death 1 ligand 1; CCL2, C-C motif chemokine ligand 2; ChIP, chromatin immunoprecipitation.

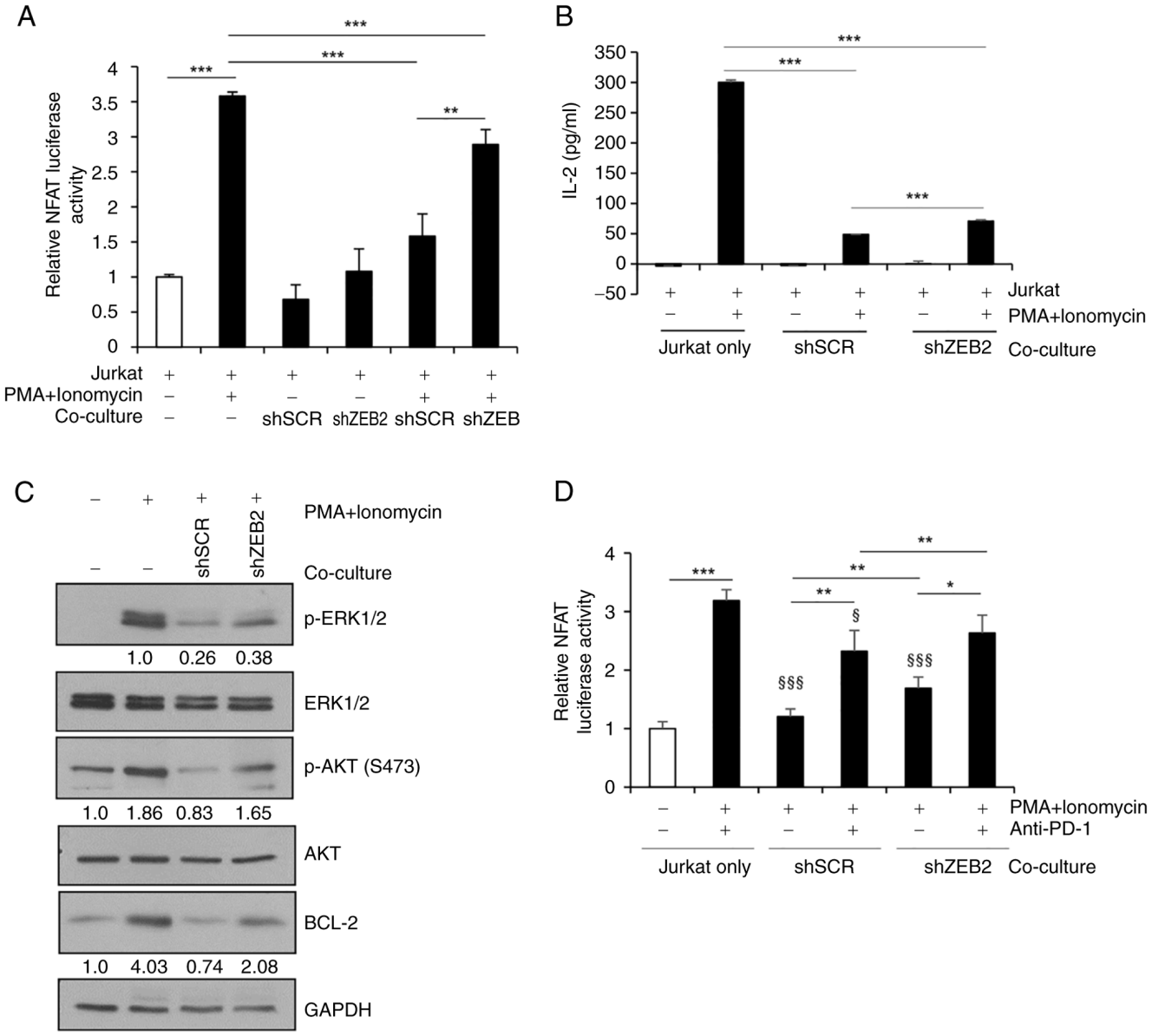

Figure 3. ZEB2 suppresses T cell activation by upregulating PD-L1. (A) Jurkat cells transfected with NFAT-reporter construct were co-cultured for 24 h with stable SNU-398 cells (control vs. ZEB2-suppressed cells) and luciferase activity was measured 24 h after stimulation with PMA and ionomycin (n=4). (B) IL-2 secreted by Jurkat cells co-cultured with stable SNU-398 cells was measured in an ELISA (n=3). (C) Jurkat cells were co-cultured for 24 h with stable SNU-398 cells and then stimulated for 24 h with PMA and ionomycin prior to immunoblot analysis. Densitometric quantification of bands on the immunoblot was performed, with GAPDH as a loading control. Phosphorylated proteins were normalized against the corresponding total protein values. (D) Effect of an anti-PD-1 antibody on NFAT activity in Jurkat cells co-cultured with stable SNU-398 cells (n=4). Values represent mean ± SD. *P<0.05; **P<0.01; ***P<0.001. $^{\$\$\$}$P<0.001 vs. Jurkat + PMA + ionomycin. ZEB2, Zinc Finger E-Box Binding Homeobox 2; PD-L1, programmed cell death 1 ligand 1; NFAT, Nuclear factor of activated T cells; ELISA, enzyme-linked immunosorbent assay; PMA, phorbol 12-myristate 13-acetate; p-, phosphorylated; sh, short hairpin.

EKR1/2 and AKT, as well as expression of BCL-2. These effects decreased to a greater extent following co-culture with control SNU-398 cells than following co-culture with ZEB2-suppressed cells (Fig. 3C).

In addition, NFAT activity in Jurkat cells decreased upon co-culture with ZEB2-expressed control SNU-398 cells; this effect was reversed markedly following addition of a PD-1-blocking antibody (Fig. 3D), indicating that PD-L1 was a critical mediator of NFAT inactivation in Jurkat cells. Meanwhile, the antibody increased NFAT activity in Jurkat cells cultured with ZEB2-suppressed SNU-398 cells, an effect probably due to residual PD-L1 expression by ZEB2-suppressed cells.

ZEB2 promotes macrophage migration and polarization by upregulating CCL2. To characterize CCL2 activity induced by ZEB2, the present study used an *in vitro* model of tumor-associated macrophages. The human monocyte cell line THP-1 was induced to differentiate into macrophages by treatment with PMA for 24 h. The macrophages were then allowed to migrate toward conditioned medium derived from either ZEB2-suppressed stable SNU-398 cells or control cells. Chemotaxis of THP-1-derived macrophages (PMA-activated THP-1 cells) was not enhanced by VEGF, but was enhanced markedly by CCL2 (50 ng/ml). Migration was also enhanced to a greater extent by conditioned medium from control cells than by conditioned medium from ZEB2-suppressed

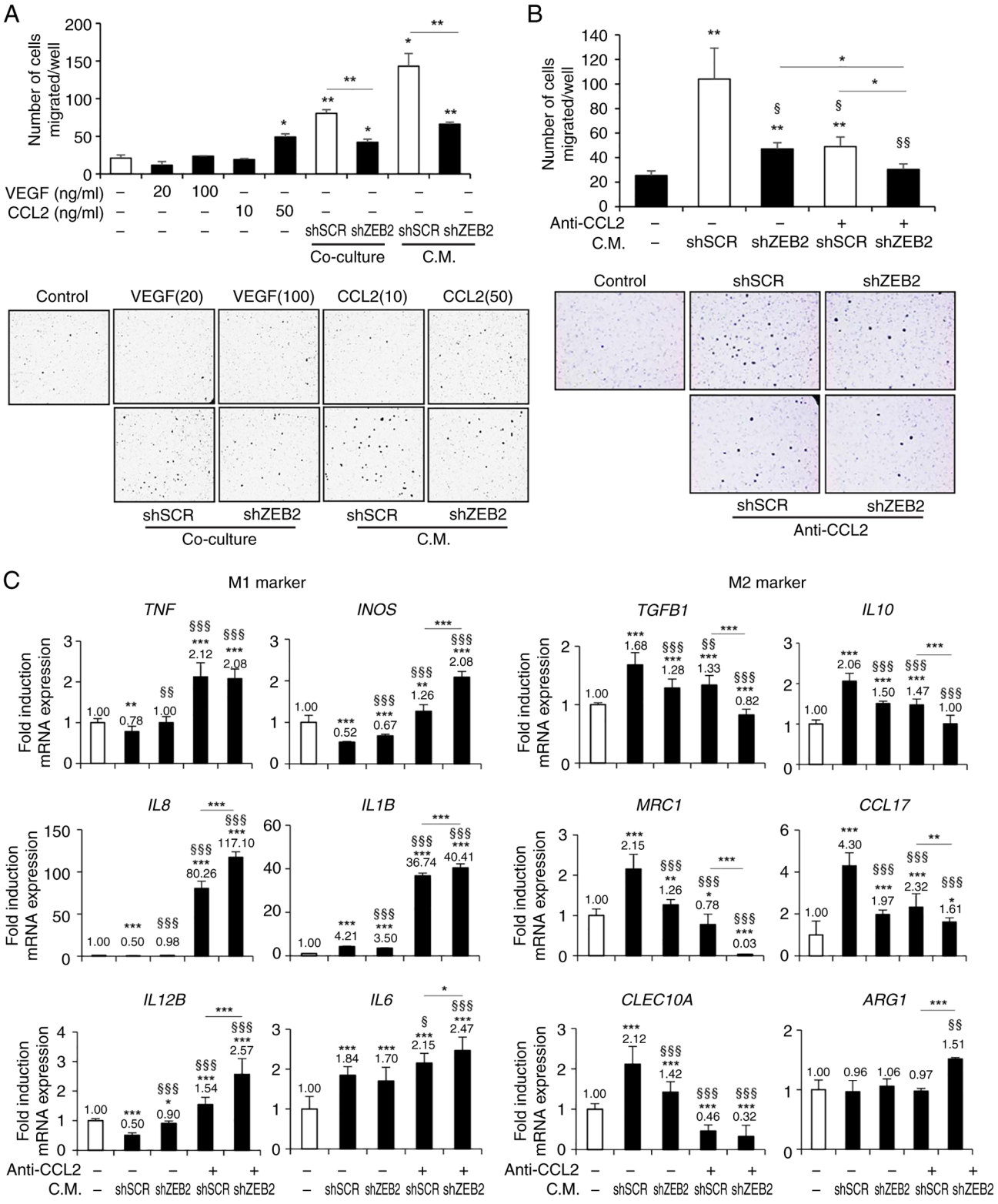

Figure 4. ZEB2 promotes macrophage migration and polarization in a CCL2-dependent manner. (A) Migration of THP-1-derived macrophages by conditioned medium from and co-culturing with stable SNU-398 cells (control vs. ZEB2-suppressed cells) (n=4). CCL2 was used as a positive control. *P<0.05; **P<0.01. (B) Migration of THP-1-derived macrophages toward conditioned medium from stable SNU-398 cells in the presence of an anti-CCL2 antibody (n=4) *P<0.05; **P<0.01 vs. no antibody + no conditioned medium; $^{\$}$P<0.05; $^{\$\$}$P<0.01 vs. no antibody + shSCR conditioned medium. (C) RT-qPCR of M1 (*TNF*, *CXCL8*/*IL8*, *IL12B*, *NOS2*/*INOS*, *IL1B* and *IL6*) and M2 (*TGFB1*, *IL10*, *MRC1*, *CLEC10A*, *CCL17* and *ARG1*) markers secreted by THP-1-derived macrophages incubated with conditioned medium from stable SNU-398 cells in the absence and presence of an anti-CCL2 antibody (n=4). *P<0.05; **P<0.01; ***P<0.001, vs. no antibody + no conditioned medium; $^{\$}$P<0.05; $^{\$\$\$}$P<0.001, vs. no antibody + shSCR conditioned medium. Values represent mean ± SD. ZEB2, Zinc Finger E-Box Binding Homeobox 2; CCL2, C-C motif chemokine ligand 2; sh, short hairpin.

cells (Fig. 4A). Chemotaxis of THP-1-derived macrophages was also promoted to a greater extent by control cells than by ZEB2-suppressed cells added to the lower chamber of the Transwell (two-chamber co-culture system; Fig. 4A).

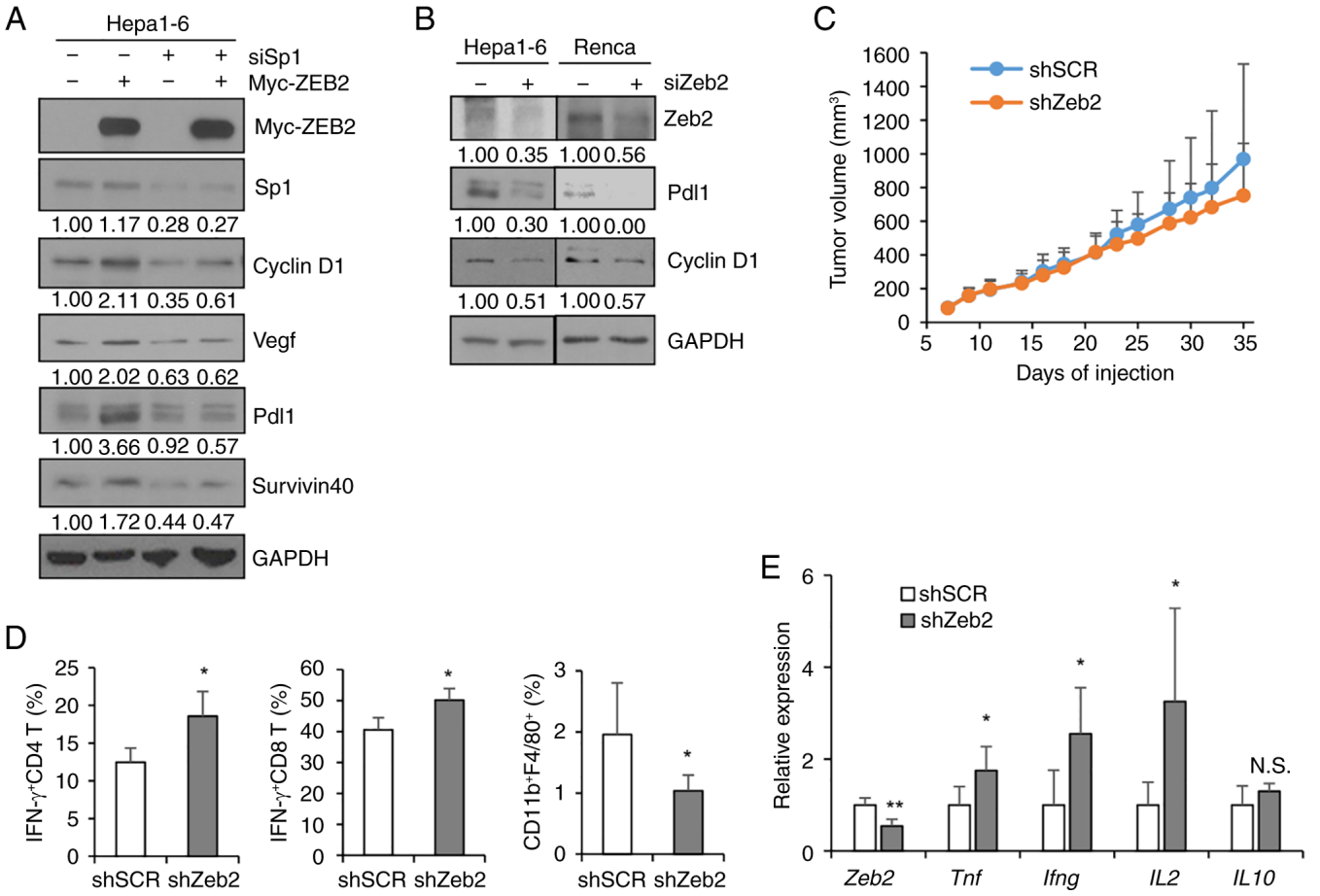

Figure 5. ZEB2 suppresses the activity of tumor-infiltrating T cells *in vivo*. (A) Cells were co-transfected for 48 h with a ZEB2 expression vector and siRNA specific for *Sp1* prior to lysis and immunoblot analysis. (B) Effect of Zeb2 suppression. Densitometric quantification of bands on the immunoblot was performed, with GAPDH as a loading control. (C) Hepa1-6 stable cells (Zeb2-suppressed vs. control cells; $1x10^7$ cells/mouse) were injected subcutaneously into the flanks of syngeneic C57BL/6 mice (n=5 per group). Tumor volume (0.5 x length x width x height) was measured for 35 days. The maximum tumor volume was 1,790 mm^3, with a length of 21 mm, on Day 35. (D) Digested tumors were analyzed for the population of IFN-γ-producing CD4 or CD8 T cells and macrophages ($CD11b^+$ $F4/80^+$) by flow cytometry after gating on $CD45^+$ cells (n=5). (E) Expression of *Zeb2* and cytokines in the tumors was measured by RT-qPCR (n=5). Values represent mean ± SD. $^*P<0.05$; $^{**}P<0.01$; N.S, not significant. ZEB2, Zinc Finger E-Box Binding Homeobox 2; sh, short hairpin; RT-qPCR, reverse transcription-quantitative PCR.

Furthermore, migration of THP-1-derived macrophages was markedly reduced following addition of a CCL2-blocking antibody to conditioned medium from ZEB2-expressing cells (Fig. 4B), suggesting that CCL2 is a critical secreted mediator of monocyte recruitment induced by ZEB2. Of note, addition of a CCL2-blocking antibody to the conditioned medium from ZEB2-suppressed cells also partially reduced migration of THP-1-derived macrophage, a finding probably due to residual CCL2 produced by ZEB2-suppressed cells, although the possibility that cytokines other than CCL2 may be involved cannot be excluded.

The present study then investigated whether stable SNU-398 cells (control vs. ZEB2-suppressed) modulated polarization of THP-1-derived macrophages. Tumor-infiltrating macrophages in most mouse and human tumors are thought to be an M2-type population (25). To examine this, THP-1-derived macrophages were incubated with conditioned medium from ZEB2-suppressed cells or control cells, followed by measurement of mRNAs encoding pro-inflammatory and anti-inflammatory cytokine by RT-qPCR. The data showed that, compared with ZEB2-suppressed cells, levels of mRNA encoding pro-inflammatory M1-type cytokines (*TNF*, *IL8*, *IL12B* and *INOS*, but not *IL1B* and *IL6*) decreased, whereas those encoding anti-inflammatory M2-type cytokines (*TGFB1*, *IL10*, *MRC1*, *CLEC10A* and *CCL17*, but not *ARG1*) increased, following treatment with conditioned medium from control cells (Fig. 4C). Polarization of THP-1-derived macrophages was reversed by addition of a CCL2-blocking antibody to the conditioned medium from ZEB2-expressing control cells (Fig. 4C). Taken together, these results suggested that ZEB2 mediates recruitment of macrophages and promotes polarization to an M2-like phenotype, mainly through upregulation of CCL2.

ZEB2 suppresses the activity of tumor-infiltrating T cells in vivo. To evaluate the effect of ZEB2 on tumor growth and immune cell activity *in vivo*, the present study first examined cooperation between ZEB2 and SP1 in mouse tumor cell lines. Transient transfection of Hepa1-6 (Fig. 5A) and Renca (Fig. S2D) cells with a ZEB2 expression vector upregulated expression of Pdl1 and survivin in Hepa1-6 cells and expression of Vegf and cyclin D1 in both cell lines. These effects

were reduced substantially by suppression of Sp1 (Fig. 5A and Fig. S2D). Next, the present study attempted to establish ZEB2-overexpressing stable cells using a Lentiviral system; however, this was not successful, possibly due to the large size of the ZEB2 expression vector (>12.7 kb). Transient suppression of Zeb2 in Hepa1-6 and Renca cells reduced expression of Pdl1 and cyclin D1 (Fig. 5B). Next, the present study generated stable Zeb2-suppressed Hepa1-6 cells, which were then injected subcutaneously into the flanks of syngeneic immunocompetent C57BL/6 mice. Although tumor growth rates were not markedly different, tumors in mice injected with Zeb2-suppressed cells (Zeb2-low) tended to grow more slowly than those in mice injected with control cells (Zeb2-high; Fig. 5C); however, flow cytometry analysis of tumors showed that tumor-infiltrating IFN-γ^+ CD8 and CD4 T lymphocytes were more common in Zeb2-low tumors than in Zeb2-high tumors (Fig. 5D left, middle). Zeb2-high tumors contained a higher number of macrophages relative to Zeb2-low tumors (Fig. 5D right). Consistent with this, RT-qPCR showed that expression of *Tnf*, *Ifng* and *IL2* in Zeb2-low tumors was higher than that in Zeb2-high tumors, with no significant difference in expression of *IL10* (Fig. 5E). There results suggested that ZEB2 tends to render tumor cells less susceptible to immune attack.

SUMOylation of ZEB2 by PC2 is required for upregulation of SP1-regulated gene expression and for subsequent cancer cell survival and invasion. SUMOylation is a protein modification that adds small ubiquitin-like modifier (SUMO) to lysine residues. ZEB2 is covalently modified by SUMOylation at two conserved sites: K391 and K866 (26). In addition, SUMOylation of ZEB2 regulates its transcriptional suppressive activity in a promoter context-dependent manner (26). Polycomb protein PC2 acts as a SUMO E3 ligase for ZEB2 (26). The present study investigated whether SUMOylation of ZEB2 modulated cooperation between ZEB2 and SP1 and thus expression of SP1-regulated genes. First, the present study generated a ZEB2 double mutant in which the two SUMOylation sites at K391 and K866 were substituted with arginine; SUMOylation was then examined. Immunoblot analysis of lysates derived from 293E cells transfected with a ZEB2 wild type or double mutant vector and treated with NEM (a deSUMOylation inhibitor) showed that wild-type ZEB2 displayed a slow migrating band of ~230 kDa, which is higher than the calculated molecular mass (170 kDa for Myc-tagged wild-type ZEB2), while the ZEB2 double mutant (K391/866R) did not display any detectable slow migrating band (Fig. S3A). These data confirmed that ZEB2 can be modified by SUMOylation at K391 and K866. Co-transfection of wild-type ZEB2, but not the ZEB2 double mutant and SUMO1 (strongly), SUMO2 and SUMO3 (moderately) increased the density of the 230 kDa slow migrating band (Fig. S3B), confirming that the 230 kDa band is a SUMO-modified form of the ZEB2 wild type. The SUMOylated form of endogenous ZEB2 was also detected in lysates derived from SNU-398 cells (Fig. S3C).

Next, the present study transiently transfected SW480 cells with wild-type ZEB2 or a ZEB2 mutant (K391/866R) expression vector prior to immunoblot analysis, invasion assays and cell survival assays. Immunoblot analysis revealed that, compared with the wild type, the ZEB2 SUMOylation null mutant (K391/866R) did not substantially upregulate expression of SP1 or SP1-regulated genes such as integrin α5, vimentin, survivin, BCL-2, VEGF, PD-L1 and CCL2. It was also confirmed that the ZEB2 mutant was expressed at a level similar to the ZEB2 wild type (Fig. 6A). The ZEB2 mutant reduced expression of E-cadherin to a lesser extent than the ZEB2 wild type (Fig. 6A). Reporter assays demonstrated that the ZEB2 wild type, but not the ZEB2 mutant, activated the *ITGA5* (integrin α5), *VIM* (vimentin), *VEGF*, *CD274* and *CCL2* promoters substantially. *CDH1* (E-cadherin) promoter activity was reduced by wild-type ZEB2 and by the ZEB2 mutant, albeit to a lesser degree (Fig. 6B). Consistent with this, wild-type ZEB2 increased invasion to a much greater extent than the ZEB2 mutant (Fig. 6C). The ZEB2 wild type, but not the ZEB2 mutant, increased cell survival markedly when transfected cells were incubated for 72 h under suspension culture conditions (Fig. 6D). An anchorage-independent growth soft agar assay showed that the ZEB2 wild type led to a modest increase in the total number of colonies while the mutant did not (Fig. 6E); however, neither the wild type nor the mutant increased the number of colonies with a diameter >0.1 mm (data not shown), suggesting that ZEB2 had limited capacity to drive anchorage-independent growth.

The role of PC2, which acts as a SUMO E3 ligase for ZEB2 (26), was then examined in ZEB2-mediated gene expression. The ZEB2 wild type upregulated expression of SP1, integrin α5, VEGF, cyclin D1, vimentin, PD-L1 and CCL2; these effects were reduced substantially following suppression of PC2 (Fig. 6F). These results suggest that SUMOylation of ZEB2 by PC2 is critical for cooperation between ZEB2 and SP1 in regulating gene expression.

SUMOylation of ZEB2 is necessary for cooperation between ZEB2 and SP1. Previously, we demonstrated that binding of ZEB2 to SP1 increases the stability of the SP1 and induces its nuclear localization (15). In addition, we showed that suppressing SP1 reduces expression of the ZEB2 protein (in both the cytoplasm and nucleus) (16), suggesting the presence of a positive feedback loop between ZEB2 and SP1. Therefore, how SUMOylation of ZEB2 affects cooperation between ZEB2 and SP1 was explored. Consistent with the results of the immunoblot analyses (Fig. 6A and F), reporter assays showed that, compared with the wild type, the ZEB2 mutant did not substantially activate a SP1 cis-element reporter plasmid (TATA-SP1 reporter) in SW480 cells (Fig. 7A). The ZEB2 wild type activated SP1 reporter activity markedly, an effect that was reduced substantially following suppression of PC2 (Fig. 7B).

To examine stability of the SP1 protein, SW480 cells were transfected with wild-type ZEB2 or ZEB2 mutant vector and then treated with a translation inhibitor, cycloheximide. Compared with the ZEB2 mutant, wild-type ZEB2 sustained expression of SP1 through increased stability of the protein (Fig. 7C). In addition, the ZEB2 mutant was less stable than the wild-type ZEB2, suggesting that stabilizing SP1 also stabilizes ZEB2. Furthermore, subcellular fractionation and immunoblot analyses showed that the ZEB2 mutant did not induce SP1 nuclear localization as efficiently as the wild type

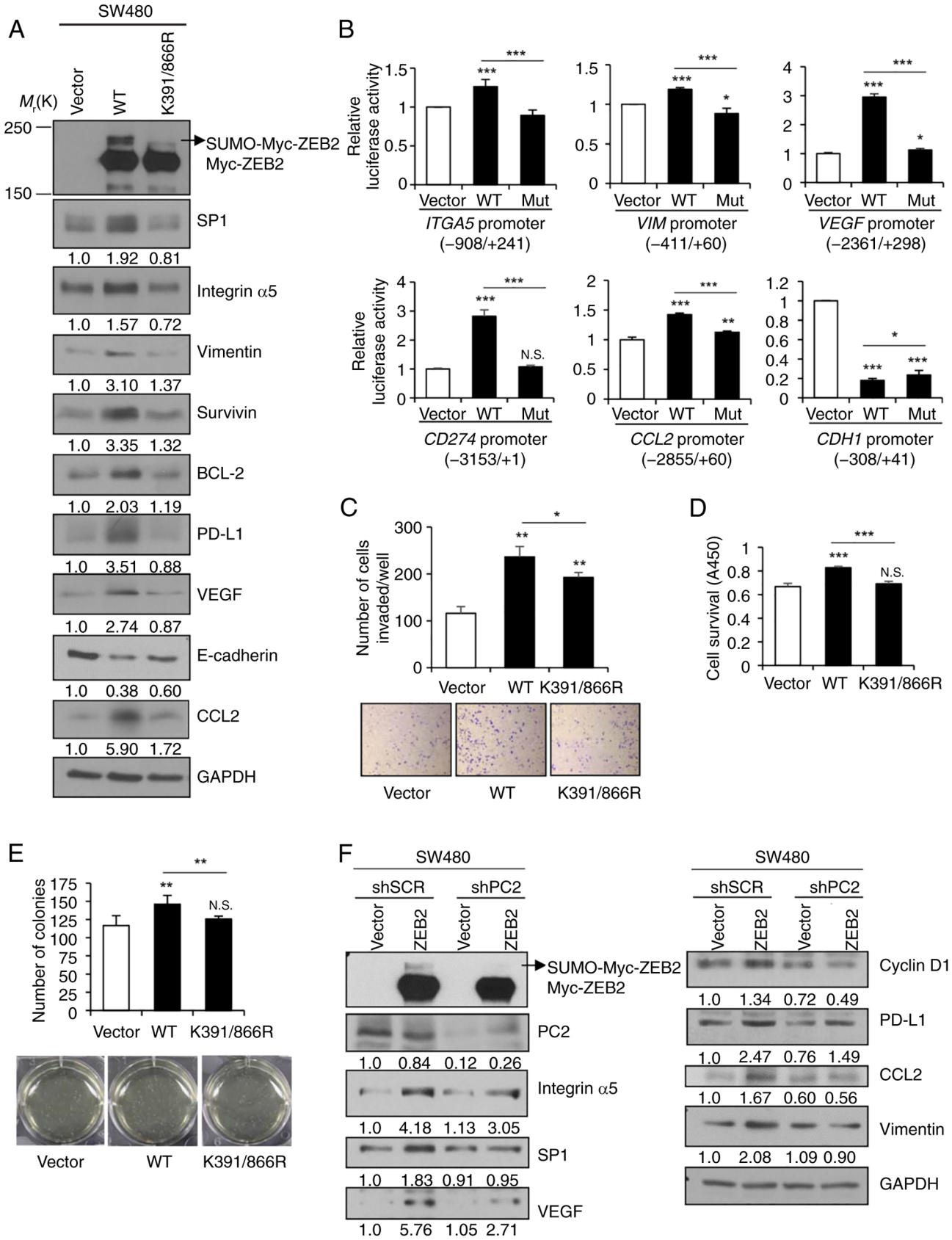

Figure 6. ZEB2 SUMOylation through PC2 is required for ZEB2 acting as a transcriptional activator and playing subsequent cellular functions. (A) SW480 cells were transfected with ZEB2WT and ZEB2_K391/866R for 48 h prior to lysis and immunoblot analysis. (B) Reporter assay of *ITGA5* (integrin α5), *VIM* (vimentin), *VEGFA*, *CDH1*, *CD274* and *CCL2* promoter activity in SW480 cells transfected with ZEB2WT and ZEB2_K391/866R (n=4). (C) Invasion (representative fields at magnification, x100), (D) survival and (E) anchorage-independent growth of SW480 cells transfected with ZEB2WT and ZEB2_K391/866R (n=3). (F) SW480 cells were co-transfected with shRNA specific for *CBX4* (shPC2) and with a ZEB2-expression vector, for 48 h prior to lysis and immunoblot analysis. Densitometric quantification of bands on the immunoblot was performed, with GAPDH as a loading control. Values represent mean ± SD. *P<0.05; **P<0.01; ***P<0.001; N.S, not significant. ZEB2, Zinc Finger E-Box Binding Homeobox 2; SUMO, small ubiquitin-like modifier; CCL2, C-C motif chemokine ligand 2; PD-L1, programmed cell death 1 ligand 1; VEGF, vascular endothelial growth factor; sh, short hairpin; WT, wild type; Mut, mutant.

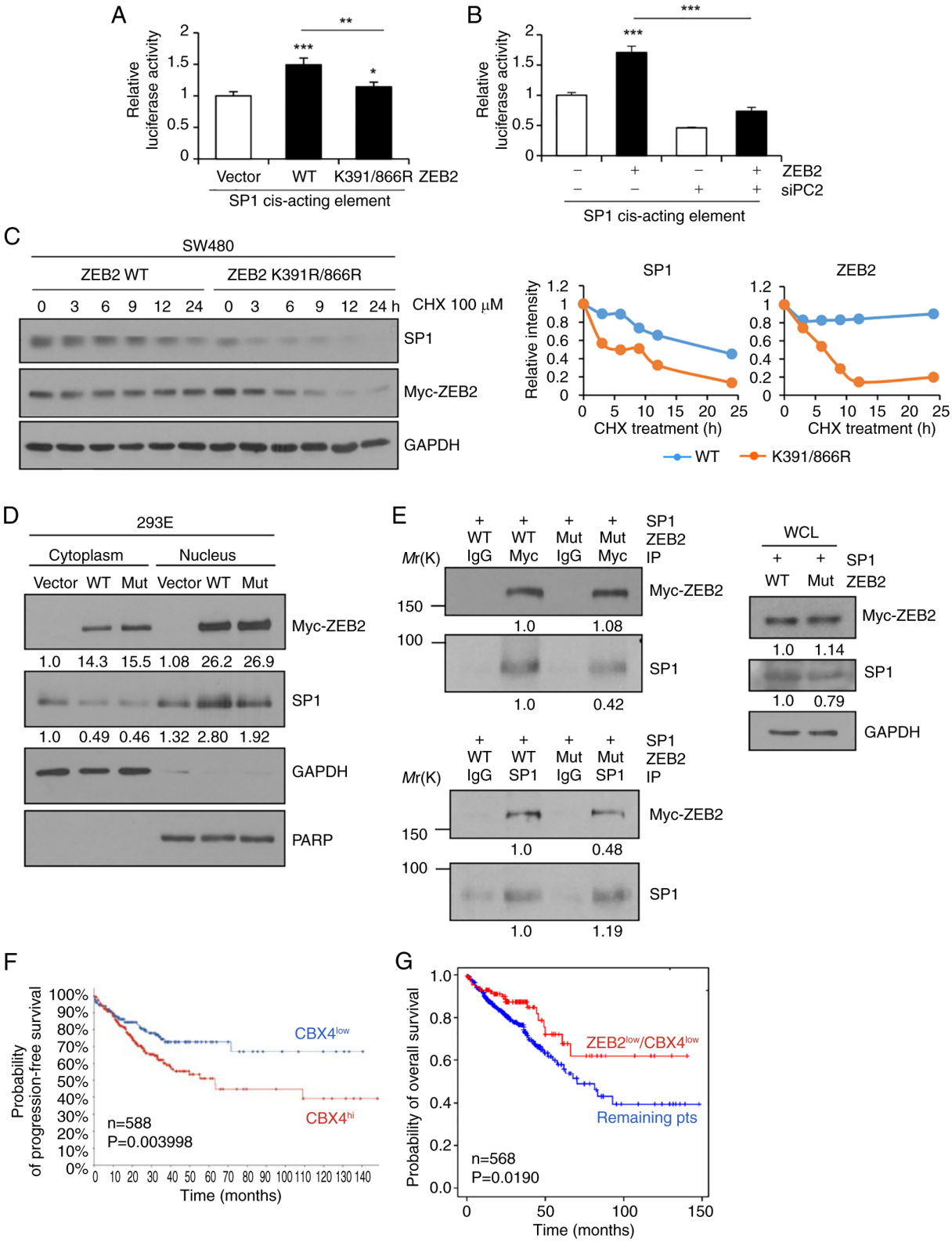

Figure 7. SUMOylation of ZEB2 is required for cooperation between ZEB2 and SP1. Reporter assay to determine transcriptional activity of SP1 in SW480 cells (n=4). (A) Cells were transfected with ZEB2WT and ZEB2_K391/866R expression vectors for 48 h. (B) Cells were co-transfected with a ZEB2 expression vector and siRNA specific for *CBX4* (siPC2) for 48 h. Values represent mean ± SD. *P<0.05; **P<0.01; ***P<0.001. (C) SW480 cells transfected with ZEB2WT and ZEB2_K391/866R expression vectors were treated with cycloheximide for the indicated times prior to lysis and immunoblot analysis. (D) A cytosolic fraction and a nuclear fraction were prepared from 293E cells transfected for 48 h with ZEB2WT and ZEB2_K391/866R expression vectors. GAPDH and PARP were used as internal controls for the cytosolic and nuclear fractions, respectively. (E) Co-immunoprecipitation analysis of the interaction between ZEB2 and SP1 in 293E cells co-transfected with ZEB2 (WT vs. K391/866R) and SP1 expression vectors. (F) Kaplan-Meier analysis showing the probability of progression-free survival of patients with colorectal adenocarcinoma (TCGA, PanCancer Atlas; n=588) in relation to *CBX4* mRNA expression. (G) Overall survival of patients with colorectal adenocarcinoma (TCGA, PanCancer Atlas; n=568) in relation to expression of *ZEB2* and *CBX4* mRNA. P-values were calculated using the log-rank test. SUMO, small ubiquitin-like modifier; ZEB2, Zinc Finger E-Box Binding Homeobox 2; CCL2, C-C motif chemokine ligand 2; PD-L1, programmed cell death 1 ligand 1; VEGF, vascular endothelial growth factor; TCGA, The Cancer Genome Atlas; si, small interfering; WT, wild type; Mut, mutant.

(Fig. 7D; lane 5 vs. 6), while ZEB2 nuclear localization was not affected substantially by SUMOylation (Fig. 7D), a finding consistent with previous observations (26).

To determine whether SUMOylation of ZEB2 affected its interaction with SP1, co-immunoprecipitation studies were performed using whole-cell lysates from 293E cells co-expressing myc-tagged ZEB2 and SP1. SP1 co-precipitated with the ZEB2 wild type, but less so with the ZEB2 mutant (Fig. 7E; upper panel). The ZEB2 wild type also co-precipitated with SP1, whereas the ZEB2 mutant co-precipitated with SP1 to a lesser extent (Fig. 7E; lower panel), suggesting that SUMOylated ZEB2 interacts efficiently with SP1.

Analysis of TCGA and GTEx datasets revealed that *CBX4* (PC2) expression is upregulated markedly in nine types of cancer, including colon, rectum and stomach cancers, compared with normal control tissues (Fig. S4). High expression of *CBX4* in colorectal adenocarcinoma patients (TCGA, PanCancer Atlas) is associated with reduced progression-free survival (Fig. 7F). In addition, low expression of both *ZEB2* and *CBX4* in colorectal adenocarcinoma (TCGA, PanCancer Atlas) correlates markedly with increased overall survival (Fig. 7G).

Discussion

Expression of EMT-TFs often correlates with increased tumor microvessel vasculature and expression of angiogenic factors (5). In addition, EMT is often accompanied by tumor immune suppression and evasion (7,8). For example, TWIST1 induces CCL2, but not VEGF and bFGF, in breast cancer cells and recruits macrophages to promote angiogenesis (27), although the molecular mechanism underlying TWIST1-induced CCL2 production remains unclear. SNAIL upregulates pro-inflammatory cytokines such as IL-6, IL-8, or CXCL1 and cyclooxygenase-2, expression of which correlates with malignancy (28). ZEB1 controls production of the IL-6 and IL-8 in breast cancer cells (29). However, the underlying molecular mechanisms remain to be determined. The present study proposed a molecular mechanism that underlies immunosuppressive activity directly mediated by EMT-TF.

Previously, we demonstrated that cooperation between ZEB2 and SP1 promotes endothelial cell activation *in vitro* and tumor angiogenesis *in vivo* by upregulating the angiogenic factor VEGF (16). The present study showed that ZEB2-SP1 cooperation upregulated CCL2 to attract macrophages. Tumor-associated macrophages promote angiogenesis by secreting angiogenic factors and proteases; therefore, it is possible that ZEB2, in cooperation with SP1, promoted angiogenesis both directly (via angiogenic factors) and indirectly (via macrophage attraction).

CCL2/MCP-1 is found in numerous types of cancer tissues, where it functions as a crucial mediator that promotes tumorigenesis and metastasis. CCL2 not only induces recruitment of monocytes/macrophages, but also contributes to establishment of an immunosuppressive microenvironment by polarizing monocytes/macrophages toward an immunosuppressive phenotype and by polarizing T lymphocytes toward a Th2 phenotype (30). For example, SNAIL+ tumor-derived CCL2 causes immunosuppression by recruiting Treg cells (31). Head and neck squamous cell carcinoma cells trigger differentiation of monocytes into M2-like macrophages by releasing CCL2 (32). Tumor-associated macrophages induce EMT programs in colorectal cancer cells, leading to production of CCL2, which in turn promotes macrophage recruitment (33). In addition, EMT is associated with M2 macrophage polarization in a MMTV-PyMT mouse model (11). TGF-β-induced overexpression of SNAIL in human THP-1 macrophages triggers M2-like differentiation by inhibiting pro-inflammatory cytokine release and promoting expression of M2-specific markers (34). The present study showed that ZEB2-mediated upregulation of CCL2 promoted macrophage migration and polarization to an M2-like phenotype. An analysis of The Tumor Immune Estimation Resource revealed that expression of ZEB2 correlated positively with neutrophil, macrophage, dendritic cell and CD8 T cell invasion and negatively with tumor-infiltrating B cell invasion, into ovarian tumors (35). In colon cancer, ZEB2 correlates with intratumoral infiltration by diverse immune cells (36). The present study also observed that ZEB2 partially upregulated expression of *CCL28*, *CXCL2*, *CXCL3*, *CXCL6* and *CXCL12,* although it did not investigate this further. It would be worth exploring the functions and significance of these ZEB2-mediated cytokines/chemokines and the underlying mechanisms, in more detail.

Over the past decades, T cell-mediated immunotherapies have emerged as promising cancer treatments. Among cancer immunotherapies, ICIs targeting PD-1 and its ligand PD-L1 display significant clinical benefits and durable responses against multiple cancer types; however, low response rates and therapeutic resistance limit the clinical benefit (8,37). Although the mechanisms underlying primary or acquired resistance to ICIs are unclear, it is suggested that post-treatment positive conversion of PD-L1 expression may be a factor (37). Increased expression of immunosuppressive cytokines such as VEGF and CCL2, along with the resulting reduction in T cell infiltration/activity in the tumor, may be associated with innate resistance to anti-PD-1 (38). TGF-β attenuates tumor responses to PD-L1 blockade by contributing to exclusion of T cells (39). In addition, EMT status is associated with activation of different immune checkpoint molecules, including PD-L1 and the EMT score may be a predictive biomarker of clinical response to ICIs (8). In addition, mesenchymal characteristics are associated with resistance to anti-PD-1 therapy. EMT status correlates with the level of PD-L1 expression on tumor cells (11); however, underlying molecular mechanisms responsible for EMT-induced PD-L1 upregulation and immunosuppression are unclear. The present study found that ZEB2 cooperated with SP1 to upregulate expression of PD-L1 and CCL2 directly, thereby inhibiting T cell infiltration/activity and macrophage attraction/polarization. ZEB2/SP1-mediated upregulated PD-L1, CCL2 and VEGF may contribute to ICI resistance; indeed, PD-L1 expression is regulated by a wide range of transcription factors, including HIF-α, c-MYC, BRD4, STAT family members, NF-κB and IRF1 (40). The present study suggested that ZEB2/SP1 transcriptionally regulated PD-L1 directly. A previous study reports that ZEB1 relieves miR-200-mediated repression of PD-L1 on tumor cells, resulting in suppression of CD8 T cells and tumor metastasis (41).

Although ZEB2 promotes EMT and metastasis, it also plays a critical cell-intrinsic role in the maturation and activation of

immune cells such as natural killer cells, cytotoxic T cells and dendritic cells, all of which play central roles in cancer immunosurveillance (7). Thus, ZEB2 plays a dual and opposing role in cancer cells compared with immune cells; ZEB2 expression in cancer cells drives initiation, dissemination, stem cell properties and resistance to therapy, whereas ZEB2 expression in the immune cells supports immunosurveillance (7,42). This duality raises concerns about potential adverse side effects of anti-tumor strategies that target ZEB2 in tumors. It would be worth investigating whether SP1 is involved in ZEB2-mediated transcriptional regulation of immune cell differentiation and maintenance. If ZEB2-SP1 cooperation is specific to tumor cells, then blocking this cooperation could suppress ZEB2 specifically in cancer cells with few adverse effects. In addition, blockade of ZEB2-SP1 cooperation may be a potential therapeutic approach to overcoming resistance to anti-PD-1/PD-L1 therapy and an immunosuppressive TME. Peptides that block interactions between interacting motifs between two proteins, or inhibitors of ZEB2 SUMOylation, may be potential therapeutics for the future.

SUMOylation regulates the functional activity of numerous transcription factors involved in EMT/MET processes, possibly because direct conjugation to SUMO alters transcriptional activity or cell trafficking (43). SUMOylation-related enzymes/factors are often upregulated in cancers and serve as potential prognostic factors (44). Development of agents targeting SUMOylation would be a novel therapeutic approach to blocking tumor growth and metastasis. Small molecule agents targeting protein SUMOylation processes (including E1, E2 and SENP) are under development as anti-cancer agents (45,46). The present study demonstrated that SUMOylation of ZEB2 by PC2 is important for cooperation between ZEB2 and SP1 and for the role of ZEB2 as a transcriptional activator that upregulates PD-L1, CCL2, VEGF, integrin α5 and survivin. This regulation is important in that the level of SUMOylation of ZEB2 may initiate or terminate cooperation between ZEB2 and SP1, as well as subsequent functions. This may contribute to modulation of EMT status (epithelial-mesenchymal plasticity) (47) to confer on cancer cells the capacity for migration, cancer stemness, or drug resistance, depending on the step of tumor progression. The present study also found that low expression of both *ZEB2* and *CBX4* correlated markedly with increased survival of patients with colorectal adenocarcinoma. Considering that the specificity of PC2 for its substrates is relatively higher than that of other SUMO E3 ligases such as PIAS (44), targeting PC2 is a potential therapeutic approach to interrupting cooperation between ZEB2 and SP1.

In summary, cooperation between SP1 and ZEB2 upregulated expression of PD-L1 on tumor cells, thereby inhibiting T cell activation, and upregulated CCL2, which in turn promoted migration of macrophages and polarization into an M2-like phenotype, thereby potentially contributing to tumor immunosuppression. Furthermore, SUMOylation of ZEB2 is required for efficient ZEB2-SP1 cooperation, subsequent gene expression and cellular functions. These findings demonstrated a previously unrecognized interplay between ZEB2, SP1, PD-L1 and CCL2, amounting to potential crosstalk between tumor cells and the tumor microenvironment during tumor progression. Taken together, the data provided evidence that immunosuppression is driven directly by an EMT-inducing transcription factor.

Acknowledgements

The authors thank Mr. J. Lee (KRIBB) and Ms. P. Seo (KRIBB) for technical assistance.

Funding

The present study was supported by grants from the National Research Foundation of Korea (grant nos. NRF-2020R1A 2C1008796 and 2023R1A2C1006554 to SK) and from the KRIBB Research Initiative Program (grant no. KGM1102511), Republic of Korea.

Availability of data and materials

The data generated in the present study are included in the figures and/or tables of this article. Other data generated in the present study may be found in the National Center for Biotechnology Information Gene Expression Omnibus (GEO) under accession number GSE293757 or at the following URL: https://www.ncbi.nlm.nih.gov/geo/query/acc.cgi?acc=GSE293757.

Authors' contributions

DK designed and performed the experiments, analyzed and interpreted the data and wrote the manuscript; YL, JY and EC performed the experiments and analyzed the data; YL, DJ and SK analyzed clinical datasets; SK designed and supervised the study, interpreted the data and wrote and revised the manuscript; DK, YL and SK confirm the authenticity of all the raw data. All authors read and approved the final manuscript.

Ethics approval and consent to participate

The animal study was performed in accordance with the guidelines of the Animal Care Committee at the KRIBB and was approved by the bioethics committee of the KRIBB (approval nos. KRIBB-AEC-22107 and KRIBB-AEC-23130).

Patient consent for publication

Not applicable.

Competing interests

The authors declare that they have no competing interests.

References

1. Lu W and Kang Y: Epithelial-mesenchymal plasticity in cancer progression and metastasis. Dev Cell 49: 361-374, 2019.
2. Thiery JP and Sleeman JP: Complex networks orchestrate epithelial-mesenchymal transitions. Nat Rev Mol. Cell Biol 7: 131-142, 2006.
3. Huang Y, Hong W and Wei X: The molecular mechanisms and therapeutic strategies of EMT in tumor progression and metastasis. J Hematol Oncol 15: 129, 2022.

4. Peinado H, Olmeda D and Cano A: Snail, Zeb and bHLH factors in tumour progression: An alliance against the epithelial phenotype? Nat Rev Cancer 7: 415-428, 2007.
5. Sanchez-Tillo E, Liu Y, de Barrios O, Siles L, Fanlo L, Cuatrecasas M, Darling DS, Dean DC, Castells A and Postigo A: EMT-activating transcription factors in cancer: Beyond EMT and tumor invasiveness. Cell Mol Life Sci 69: 3429-3456, 2012.
6. Zheng H and Kang Y: Multilayer control of the EMT master regulators. Oncogene 33: 1755-1763, 2014.
7. Goossens S, Vandamme N, Van Vlierberghe P and Berx G: EMT transcription factors in cancer development re-evaluated: Beyond EMT and MET. Biochim Biophys Acta Rev Cancer 1868: 584-591, 2017.
8. Jiang Y and Zhan H: Communication between EMT and PD-L1 signaling: New insights into tumor immune evasion. Cancer Lett 468: 72-81, 2020.
9. Hanahan D and Weinberg RA: Hallmarks of cancer: The next generation. Cell 144: 646-674, 2011.
10. Tie Y, Tang F, Wei YQ and Wei XW: Immunosuppressive cells in cancer: Mechanisms and potential therapeutic targets. J Hematol Oncol 15: 61, 2022.
11. Dongre A, Rashidian M, Reinhardt F, Bagnato A, Keckesova Z, Ploegh HL and Weinberg RA: Epithelial-to-mesenchymal transition contributes to immunosuppression in breast carcinomas. Cancer Res 77: 3982-3989, 2017.
12. Hugo W, Zaretsky JM, Sun L, Song C, Moreno BH, Hu-Lieskovan S, Berent-Maoz B, Pang J, Chmielowski B, Cherry G, *et al*: Genomic and transcriptomic features of response to anti-PD-1 therapy in metastatic melanoma. Cell 165: 35-44, 2016.
13. Dong P, Xiong Y, Yue J, Hanley SJB and Watari H: Tumor-intrinsic PD-L1 signaling in cancer initiation, development and treatment: Beyond immune evasion. Front Oncol 8: 386, 2018.
14. Nam EH, Lee Y, Park YK, Lee JW and Kim S: ZEB2 upregulates integrin alpha5 expression through cooperation with Sp1 to induce invasion during epithelial-mesenchymal transition of human cancer cells. Carcinogenesis 33: 563-571, 2012.
15. Nam EH, Lee Y, Zhao XF, Park YK, Lee JW and Kim S: ZEB2-Sp1 cooperation induces invasion by upregulating cadherin-11 and integrin alpha5 expression. Carcinogenesis 35: 302-314, 2014.
16. Ko D and Kim S: Cooperation between ZEB2 and Sp1 promotes cancer cell survival and angiogenesis during metastasis through induction of survivin and VEGF. Oncotarget 9: 726-742, 2018.
17. Jang D, Kwon H, Choi M, Lee J and Pak Y: Sumoylation of flotillin-1 promotes EMT in metastatic prostate cancer by suppressing snail degradation. Oncogene 38: 3248-3260, 2019.
18. Bonello GB, Pham MH, Begum K, Sigala J, Sataranatarajan K and Mummidi S: An evolutionarily conserved TNF-alpha-responsive enhancer in the far upstream region of human CCL2 locus influences its gene expression. J Immunol 186: 7025-7038, 2011.
19. Nam EH, Lee Y, Moon B, Lee JW and Kim S: Twist1 and AP-1 cooperatively upregulate integrin alpha5 expression to induce invasion and the epithelial-mesenchymal transition. Carcinogenesis 36: 327-337, 2015.
20. Gao J, Aksoy BA, Dogrusoz U, Dresdner G, Gross B, Sumer SO, Sun Y, Jacobsen A, Sinha R, Larsson E, *et al*: Integrative analysis of complex cancer genomics and clinical profiles using the cBioPortal. Sci Signal 6: pl1, 2013.
21. Cerami E, Gao J, Dogrusoz U, Gross BE, Sumer SO, Aksoy BA, Jacobsen A, Byrne CJ, Heuer ML, Larsson E, *et al*: The cBio cancer genomics portal: An open platform for exploring multidimensional cancer genomics data. Cancer Discov 2: 401-404, 2012.
22. Cancer Genome Atlas Network: Comprehensive molecular characterization of human colon and rectal cancer. Nature 487: 330-337, 2012.
23. Vasaikar S, Huang C, Wang X, Petyuk VA, Savage SR, Wen B, Dou Y, Zhang Y, Shi Z, Arshad OA, *et al*: Proteogenomic analysis of human colon cancer reveals new therapeutic opportunities. Cell 177: 1035-1049.e1019, 2019.
24. Simon R, Lam A, Li MC, Ngan M, Menenzes S and Zhao Y: Analysis of gene expression data using BRB-arraytools. Cancer Inform 3: 11-17, 2007.
25. Wang S, Wang J, Chen Z, Luo J, Guo W, Sun L and Lin L: Targeting M2-like tumor-associated macrophages is a potential therapeutic approach to overcome antitumor drug resistance. NPJ Precis Oncol 8: 31, 2024.
26. Long J, Zuo D and Park M: Pc2-mediated sumoylation of Smad-interacting protein 1 attenuates transcriptional repression of E-cadherin. J Biol Chem 280: 35477-35489, 2005.
27. Low-Marchelli JM, Ardi VC, Vizcarra EA, van Rooijen N, Quigley JP and Yang J: Twist1 induces CCL2 and recruits macrophages to promote angiogenesis. Cancer Res 73: 662-671, 2013.
28. Lyons JG, Patel V, Roue NC, Fok SY, Soon LL, Halliday GM and Gutkind JS: Snail up-regulates proinflammatory mediators and inhibits differentiation in oral keratinocytes. Cancer Res 68: 4525-4530, 2008.
29. Katsura A, Tamura Y, Hokari S, Harada M, Morikawa M, Sakurai T, Takahashi K, Mizutani A, Nishida J, Yokoyama Y, *et al*: ZEB1-regulated inflammatory phenotype in breast cancer cells. Mol Oncol 11: 1241-1262, 2017.
30. Gschwandtner M, Derler R and Midwood KS: More than just attractive: How CCL2 influences myeloid cell behavior beyond chemotaxis. Front Immunol 10: 2759, 2019.
31. Kudo-Saito C, Shirako H, Ohike M, Tsukamoto N and Kawakami Y: CCL2 is critical for immunosuppression to promote cancer metastasis. Clin Exp Metastasis 30: 393-405, 2013.
32. Gao L, Wang FQ, Li HM, Yang JG, Ren JG, He KF, Liu B, Zhang W and Zhao YF: CCL2/EGF positive feedback loop between cancer cells and macrophages promotes cell migration and invasion in head and neck squamous cell carcinoma. Oncotarget 7: 87037-87051, 2016.
33. Wei C, Yang C, Wang S, Shi D, Zhang C, Lin X, Liu Q, Dou R and Xiong B: Crosstalk between cancer cells and tumor associated macrophages is required for mesenchymal circulating tumor cell-mediated colorectal cancer metastasis. Mol. Cancer 18: 64, 2019.
34. Zhang F, Wang H, Wang X, Jiang G, Liu H, Zhang G, Wang H, Fang R, Bu X, Cai S and Du J: TGF- β induces M2-like macrophage polarization via SNAIL-mediated suppression of a pro-inflammatory phenotype. Oncotarget 7: 52294-52306, 2016.
35. Kim HR, Seo CW, Han SJ, Lee JH and Kim J: Zinc finger E-box binding homeobox 2 as a prognostic biomarker in various cancers and its correlation with infiltrating immune cells in ovarian cancer. Curr Issues Mol Biol 44: 1203-1214, 2022.
36. Xie H, Wu Z, Li Z, Huang Y, Zou J and Zhou H: Significance of ZEB2 in the immune microenvironment of colon cancer. Front Genet 13: 995333, 2022.
37. Wang Y, Wang H, Yao H, Li C, Fang JY and Xu J: Regulation of PD-L1: emerging routes for targeting tumor immune evasion. Front Pharmacol 9: 536, 2018.
38. Peng W, Chen JQ, Liu C, Malu S, Creasy C, Tetzlaff MT, Xu C, McKenzie JA, Zhang C, Liang X, *et al*: Loss of PTEN promotes resistance to T cell-mediated immunotherapy. Cancer Discov 6: 202-216, 2016.
39. Mariathasan S, Turley SJ, Nickles D, Castiglioni A, Yuen K, Wang Y, Kadel EE III, Koeppen H, Astarita JL, Cubas R, *et al*: TGFβ attenuates tumour response to PD-L1 blockade by contributing to exclusion of T cells. Nature 554: 544-548, 2018.
40. Yi M, Niu M, Xu L, Luo S and Wu K: Regulation of PD-L1 expression in the tumor microenvironment. J Hematol Oncol 14: 10, 2021.
41. Chen L, Gibbons DL, Goswami S, Cortez MA, Ahn YH, Byers LA, Zhang X, Yi X, Dwyer D, Lin W, *et al*: Metastasis is regulated via microRNA-200/ZEB1 axis control of tumour cell PD-L1 expression and intratumoral immunosuppression. Nat Commun 5: 5241, 2014.
42. Scott CL and Omilusik KD: ZEBs: Novel players in immune cell development and function. Trends Immunol 40: 431-446, 2019.
43. Bogachek MV, De Andrade JP and Weigel RJ: Regulation of epithelial-mesenchymal transition through SUMOylation of transcription factors. Cancer Res 75: 11-15, 2015.
44. Seeler JS and Dejean A: SUMO and the robustness of cancer. Nat Rev Cancer 17: 184-197, 2017.
45. Yang Y, Xia Z, Wang X, Zhao X, Sheng Z, Ye Y, He G, Zhou L, Zhu H, Xu N and Liang S: Small-molecule inhibitors targeting protein sumoylation as novel anticancer compounds. Mol Pharmacol 94: 885-894, 2018.
46. Brackett CM and Blagg BSJ: Current status of sumoylation inhibitors. Curr Med Chem 28: 3892-3912, 2021.
47. Shibue T and Weinberg RA: EMT, CSCs and drug resistance: The mechanistic link and clinical implications. Nat Rev Clin Oncol 14: 611-629, 2017.